

**3D analysis of mandibular deciduous tooth crypts using μ CT
imaging**

by

Anu Korada

BSc Biochemistry, King's College London, 1995

BDS, King's College London, 2000

A THESIS SUBMITTED IN PARTIAL FULFILLMENT OF THE REQUIREMENTS FOR

THE DEGREE OF

MASTER OF SCIENCE

in

THE FACULTY OF GRADUATE and POSTDOCTORAL STUDIES

(Craniofacial Science)

THE UNIVERSITY OF BRITISH COLUMBIA

(Vancouver)

August, 2016

© Anu Korada, 2016

Abstract

Objectives: Interactions between the dental follicle and the alveolar bone are tightly coordinated such that the correct amount of support for each tooth is formed. Prior to root formation, bone-tooth interactions may also regulate the shape or size of the crown. Here we measure the increase in tooth and mandibular volume and then go onto to determine whether growth of each crypt is allometric or isometric. Finally we determine whether tooth shape is influenced by local factors.

Methods: Fetal heads 12 to 19 weeks were obtained from BC Women's hospital (N = 25; Protocol H08-02576). Heads were scanned at 50 μ m resolution, reconstructed and segmented using Amira v5.6 software. Statistical analysis included two-way ANOVA and post-hoc Tukey's test. Landmark and Morpho J software was used for landmark-based geometric morphometrics.

Results: Segmentation of the mandible and crypts revealed that the alveolar bone varied according to the tooth type, surface and age of specimen. The patterns of bone were symmetrical within each specimen. The typical pattern consisted of 1) absence of occlusal bone, 2) presence of gingival bone, 3) interproximal bone on the mesial and distal of the c, 4) varying degrees of buccal bone on the c and m1. Volumetric measurements revealed 3 periods of growth - 12-14 weeks, 15-16 weeks and 17-19 weeks. 3D morphometrics revealed that the buccal landmarks of m1 and c were displaced buccally, gingival landmarks for i1, i2 and c were displaced gingivally and distal landmarks on m2 were displaced mesially.

Conclusions: The surprising regional differences in the presence of bone on different sides of the follicle suggests that there must be local signaling mechanisms at work. The high degree of symmetry between the right and left sides further suggests that these regional patterning mechanisms are controlled by genetic rather than environmental mechanisms.

Preface

Whole human fetal heads were kindly provided by Dr V Diewert (Professor of Orthodontics at UBC) (Human ethics protocol H08-02576). The fetuses were obtained as a result of elective terminations carried out at BC Women's Hospital from 1986 to 1988.

Funding was obtained from the Faculty of Dentistry awarded to JMR and Faculty of Dentistry. Pilot Project grant to Dr V Diewert.

Design of the study was by Dr Richman and Dr Anu Korada.

The μ CT scans were carried out by John Schipilow (Lab technician) at the Centre for High Throughput Phenogenomics.

Instruction on the use of the FEI Amira 5.6 was given by technicians at the CHTP or the Bioimaging department UBC. The use of Landmark, Morpho J and Statistica was instructed by Dr Richman. All data collection and analyses were done by Dr Anu Korada under the supervision of Dr. Richman.

Table of contents

Abstract	i
Preface	ii
Table of Contents.....	iv
List of Tables	vii
List of Figures	viii
List of Abbreviations	ix
Acknowledgements	x
Dedication.....	xi
CHAPTER 1: Introduction	1
1.1 Embryonic facial growth	1
1.1.1 Neural crest migration and facial prominences	1
1.1.2 Development of the chondrocranium	2
1.1.3 Intramembranous ossification	3
1.1.4. Tooth Development during the late embryonic and fetal periods	4
1.2 3D studies of craniofacial growth.....	8
1.3 Hypotheses.....	9
1.4 Aims.....	9

Chapter 2: Material and Methods	11
2.1 Origin of the specimens	11
2.2 Micro computed tomography scanning.....	13
2.3 Segmentation of the mandible and tooth crypts.....	13
2.4 Measurements.....	16
2.5 The landmark based software Morpho J to analyse shape changes.....	21
2.6 Statistics analysis.....	21
Chapter 3: Results.....	23
3.1. Alveolar bone morphogenesis	25
3.2. Buccal plate fenestration is highly variable in the mandibular dentition	28
3.3. Quantification of mandibular volume and variability in the sample	32
3.4. Tooth crypt volume.....	39
3.5. Tooth crypt dimensions.....	41
Chapter 4: Discussion.....	52
4.1 Micro-CT imaging reveals temporal and spatial changes in fenestration of the buccal bone, and septation between crypts.....	52
4.1.1 Interactions between adjacent tooth follicles	55

4.1.2	Growth of tooth crypts is proportionate to mandibular growth but not linear	55
4.2	Is the mandibular bone controlling the shape of the follicle or vice versa?	57
4.3	Limitations of the study	58
4.4	Future directions.....	60
4.4.1	Standard μ CT does not document the soft tissues.....	60
4.4.2	Genetic control of dental crowding	62
Bibliography		63
Appendix A: Buccal bone description by specimen on right and left sides.....		66

List of Tables

Table 2.1	Characteristics of the fetuses used in the study	12
Table 2.2	Location of homologous landmarks on tooth crypt volume renderings	20
Table 3.1	Buccal Fenestration phenotype by specimen	30
Table 3.2	Reproducibility of segmentation as shown by repeated measurements of canine crypts	38
Table 3.4	Percentage increase in volume and dimensions between the average 12 week and average 19 week specimens	47

List of Figures

Figure 1.1	Illustration from (Ooë, 1981) with follicles and bony crypts in a 14 wk human fetus.....	5
Figure 2.1	Segmentation method to mark the boundaries of the crypts within the mandibular bone	15
Figure 2.2	Location of measurement landmarks for standard morphometrics	17
Figure 2.3	Homologous landmarks	19
Figure 3.1	Isosurfaces of whole human fetal skulls from 12-19 weeks	24
Figure 3.2	Segmented mandibular bone reveals formation of the septae between crypts	27
Figure 3.3	Relationship between the buccal bone and the tooth crypts is highly variable	31
Figure 3.4	Distribution of specimens by week gestation, mandibular volume and CRL	34
Figure 3.5	Shapiro-Wilks test of normality.....	36
Figure 3.6	Volumetric measurements.....	40
Figure 3.7	Incisogingival length changes between 12 and 19 weeks	44
Figure 3.8	Buccolingual length changes between 12 and 19 weeks.....	45
Figure 3.9	Mesiodistal length.....	46
Figure 3.10	Principal component analysis.....	50
Figure 3.11	Discriminant function analysis with wireframe graphical output showing shape changes.....	51
Figure 4.1	Comparison of microCT imaging before and after PTA staining	61

List of Abbreviations

ANOVA: Analysis of Variance

BL: Bucco-Lingual

c: Primary canine

CRL: Crown rump length

CVA: Canonical Variate Analysis 3D: 3- dimensional

2D: 2-dimensional

DFA: Discriminant Function Analysis

DICOM: Digital imaging and communication in Medicine EO: Enamel organ

HC: Head Circumference i1: Primary central incisor i2: Primary lateral incisor IG: Incio-
Gingival

m1: Primary first molar m2: Primary second molar MD: Mesio-Distal

PCA: Principal Component Analysis PC1: Principal Component 1

PC2: Principal Component 2 PTA: Phosphotungstic acid

μ CT: Micro computed tomography UBC: University of British Columbia

Wnt: Wingless-type MMTV integration site family member

Bmp: Bone morphogenic proteins

Acknowledgements

I would like to thank Dr Richman for her help and support in completing my thesis without her help I would not been able to finish.

I would like to thank Dr Diewert for providing the unique samples and for being part of my committee member and her continuous interest and enthusiasm.

I would like to thank Dr Ford for being my committee member and offering her input and support.

Thank you very much to John Schipilow for all his help with Amira without him Amira would have been even more challenging.

And a special thank you to my children Adesh and Ashwin and my husband Murthy, for putting up with my absence.

Dedication

Dedicated to my husband Murthy, my children Adesh and Ashwin and my parents without whom this would not have been possible.

CHAPTER 1: Introduction

1.1 Embryonic facial growth

1.1.1 Neural crest migration and facial prominences

Facial development begins with neural crest cell migration. Neuroectoderm cells that were originally part of the neural plate begin to separate and migrate into the head mesoderm. There neural crest cells transform from ectoderm to mesenchyme as they leave the dorsal edges of the cranial neural plate or presumptive brain. As the neural tube closes and folds up to form the brain, streams of neural crest cells enter the future face which is forming on the ventral side of the embryo (O'Rahilly and Muller, 2007; Radlanski et al., 2016). Migration of neural crest cells is at its peak at 22-23 days or stage 10 in the Carnegie staging system. Most of the facial neural crest cells arise from the forebrain, midbrain and anterior hindbrain (O'Rahilly and Muller, 2007). The primitive stomodeum or oral cavity is initially surrounded by neural crest cells and these grow out to form buds or facial prominences. The first recognizable prominence is the first pharyngeal arch which is caudal to the stomodeum. The first pharyngeal arch gives rise to the entirety of the mandible or lower jaw. The cranial part of the first pharyngeal arch as well as mesenchyme posterior to the primitive eye (post-optic) forms the maxillary prominence (Lee et al., 2004). The maxillary prominence gives rise to most of the upper jaw skeleton including palatine bones, maxillary bones and most likely the zygomatic arch. Cranial to the stomodeum, the midline is formed by the frontonasal and medial nasal prominences (medial to the nasal pits). Lateral to the nasal pits are the lateral nasal prominences. The outgrowth and fusion of the medial nasal, lateral nasal and maxillary prominences gives rise to the lip. Lip fusion takes place between 42 and 44 days post conception or Carnegie stage 18-19 (Diewert, 1985). Skeletal derivatives of the medial nasal

prominences include the premaxilla, nasal septum and the 4 incisors of the upper jaw. The lateral nasal prominences give rise to the nasal turbinates as shown in chicken fate mapping studies (MacDonald et al., 2004). The midline merging of the medial nasal prominences is a critical event in facial morphogenesis leading to formation of a focused midline (Diewert and Wang, 1992).

1.1.2 Development of the chondrocranium

In the late embryonic period starting at week 6, the cartilagenous skull begins to differentiate (Diewert, 1985; Sperber and Guttman, 2010). The chondrocranium is the most primitive, evolutionarily conserved part of the skull. In humans, the chondrocranium is the initial support for the brain and sensory organs. The cranial base posterior to sella turcica is derived from paraxial mesoderm whereas the anterior cranial base is derived from cranial neural crest cells as determined in mouse lineage tracing studies (McBratney-Owen et al., 2008). Cranial base angle as measured between the anterior and posterior cranial base is thought to have a direct relationship to jaw relationships (Diewert and Wang, 1992). The nasal septal cartilage, nasal conchae and Meckel's cartilage are all derived from cranial neural crest cells. Growth of the nasal septum is thought to drive upper jaw growth. Importantly, Meckel's cartilage drives mandibular growth starting at 8 weeks shortly after differentiation of chondrocytes occurs. The extension of Meckel's cartilage rostrally, along with the head lifting up from the thorax, enables the tongue to move away from the palatal shelves. This timing coincides with reorientation of the palatal shelves from vertical to horizontal allowing for contact in the midline and subsequent fusion (Diewert, 1985). The mandible is transiently prognathic at 10 weeks gestation (Diewert, 1985). The human skull is

entirely composed of cartilage up until 6 weeks of fetal development (O'Rahilly and Müller, 2001; Sperber et al., 2010).

1.1.3 Intramembranous ossification

During the late embryonic period, intramembranous bone begins to condense directly from neural crest-derived mesenchyme, initiating first in the mandible between 6-7 weeks (Sperber et al., 2010). The bifurcation of the mandibular division of the trigeminal nerve into the mental and incisive branches acts as the site of the first ossification center at around 6 weeks gestation (Radlanski, 2003a; Sperber et al., 2010). The mandibular bone initiates lateral to the Meckel's cartilage and is not derived from the cartilage template. The primary ossification center eventually enlarges to form the mandibular bone which envelopes Meckel's cartilage.

The mandible appears as a single bone at birth, however developmentally it is subdivided into several skeletal units: the body of the mandible to which the alveolar bone is attached, the coronoid, angular and condylar processes and the chin. The alveolar process is formed by intramembraneous ossification and the condyle and coronoid are formed by endochondral ossification (Sperber et al., 2010). However the true alveolar process only forms after the teeth erupt. Prior to eruption the teeth are in crypts within the maxillary, premaxillary or mandibular bones (Radlanski et al., 2016). These skeletal elements are also influenced by the functional matrix that stimulates bone apposition and resorption; muscles such as the temporalis, masseter and medial pterygoid affect bone remodeling (Bareggi et al., 1995).

1.1.4. Tooth Development during the late embryonic and fetal periods

Tooth germ develops from tissues originating from both ectoderm and mesoderm at approximately 6 weeks of age. The basal layer of the fetal oral epithelium starts to enlarge in areas of the future dental arches. There is also increased activity and size on the basal layer to represent the dental lamina of the future tooth germs. There are 20 sites of the epithelial activity to represent the 20 tooth germs of the primary dentition. In addition to the developing 20 primary teeth the dental lamina for the developing permanent tooth also appears for the first time at around 19-20 weeks gestation or 160mm CRL, (Radlanski et al., 2016) . The developing primary central, lateral and canine produce dental lamina for the future respective permanent teeth and the primary molars produce the dental lamina for the future first and second bicuspid. The three permanent molars develop from the dental lamina extending distally from the second primary molar (Juuri et al., 2013; Ooë, 1981) .

Tissue interactions between the epithelium and mesenchyme are required for tooth morphogenesis. Initially the oral epithelium induces dental fate in the underlying mesenchyme (Mina and Kollar, 1987). Next the mesenchyme induces the invagination of the ectoderm to form the tooth bud and formation of a signaling center called the enamel knot (Thesleff et al., 2001). The bud passes into the cap and bell stage in which the enamel organ is comprised of 4 layers, the outer enamel epithelium, stellate reticulum, stratum intermedium and inner enamel epithelium. The dental follicle is formed during the cap stage of tooth development; it is initiated by an ectomesenchymal progenitor cell population originating from the neural crest cells. The dental follicle stem cells are the origin of the periodontium (the cementum, periodontal ligament and the alveolar bone) (Fleischmannova et al., 2010) . In addition, the dental follicle signals to the surrounding tissue resulting in the attracting of osteoclasts. The osteoclasts are

responsible for creating an eruption pathway (Wise and King, 2008). In other words, without the follicle teeth will not erupt (Cahill and Marks, 1980; Marks and Cahill, 1984) . The cells of the dental follicle are a source of mesenchymal stem cells and are capable of differentiating into cementoblasts, osteoblasts, osteoclasts, fibroblasts (Honda et al., 2011). The main signaling pathways regulating the follicle-bone interface are prostaglandins, IL-1, IL-6, TNF α , receptor activator of nuclear factor kappa B ligand (RANK/RANKL) (Wise and King, 2008).

Figure 1.1 Illustration from (Ooë, 1981) with follicles and bony crypts in a 14 wk human fetus.

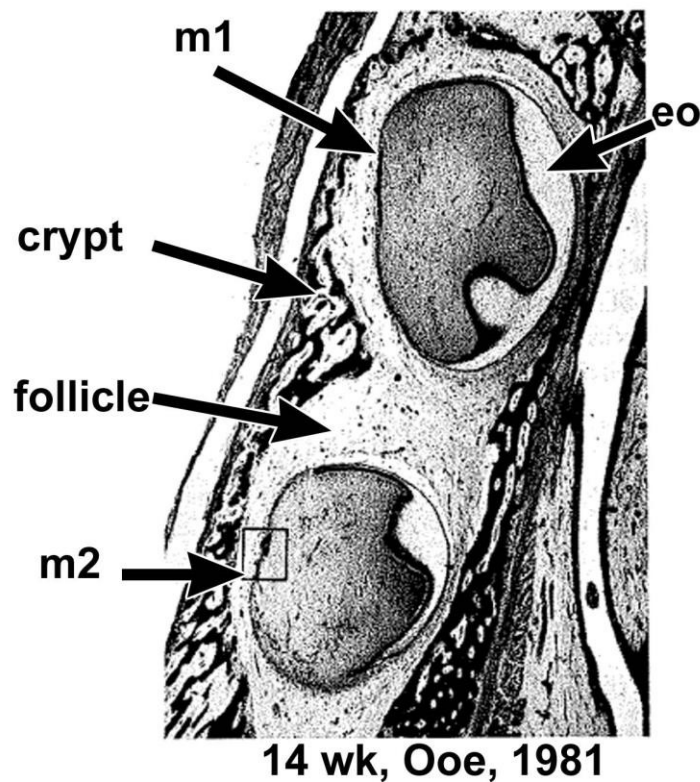


Fig. 1.1 Horizontal section of posterior mandible. The m1 and m2 molar follicles can be seen in a 14 wk human foetus. The eo is the enamel organ. The follicles are discrete entities and it can be seen that they sit in the crypt. An interdental septa cannot be seen between the m1 and m2.

In my study we are studying the tooth crypt to have a better understanding of tooth follicle development. The follicle is in direct contact with the bone during fetal development (Fig. 1.1). At 12 weeks gestation, the starting point for our study, fetuses are between 87mm to 89mm CR. Teeth are in the bud stage (Radlanski et al., 2016). At 14 weeks or 103-105mm CRL, teeth reach bell stage of development (Dong et al., 2014; Wang et al., 2014) . The dental organ has differentiated into the inner and outer dental epithelium, stellate reticulum and stratum intermedium. At 14 weeks the dental lamina of the secondary tooth becomes more obvious as an extension. There are some recent studies examining expression of genes in human fetal teeth between 12 and 14 weeks (Dong et al., 2014; Wang et al., 2014). *BMP3* was detected in the mesenchymal cells, the dental papilla and dental sac that give rise to osteoclasts, osteoblasts and cementoblasts. Several *WNT* genes are expressed in the enamel organ. In addition the canonical WNT pathway mediator, beta-catenin is especially highly expressed in the enamel knot (Wang et al., 2014). These expression patterns illustrate that there is signaling taking place in the enamel organ similar to what has been described in the mouse.

At 16 weeks or 149mm CRL the tooth germ is in late bell stage, (Radlanski et al., 2016) . The cells of the inner enamel epithelium induce the odontoblasts. Then the first layer of dentin is deposited which leads to differentiation of ameloblasts. The first enamel is deposited at the cusp tips, the locations of the enamel knots (Balic and Thesleff, 2015; Thesleff et al., 2001). At 17 weeks or 160 mm CRL gestation the tooth germ is in the late bell stage and mineralizing enamel can be detected. The cervical loops are extending to complete the crown.

Further histodifferentiation and root development of the primary teeth continues after birth (Logan and Kronfeld, 1933).

The permanent teeth also initiate prenatally in the middle trimester. The first permanent molar initiates at 17 weeks (Ooë, 1981; Radlanski et al., 2016). The buds of the permanent canine and incisors are visible on the lingual surfaces of the primary teeth at 225 mm CRL (23-24 weeks) (Ooë, 1981; Radlanski et al., 2016). Thus starting in the 23rd week the crypts of the primary teeth contain the buds of second generation teeth.

1.2 3D studies of craniofacial growth

The tooth-bone interface is being established in the fetal period. However, there is a paucity of 3D studies on human fetal jaws. To obtain 3D information, histological sections were made, then tracings made using a camera lucida, the tracings were stacked up so that structures aligned and then models were reconstructed using wax (Blechs Schmidt, 1953; Norberg, 1933) or stacks of cardboard (Ooë, 1981). Many papers by Radlanski used computer-aided reconstruction and focused on embryos up to 8 weeks gestation (Radlanski, 1995; Radlanski, 2003a; Radlanski, 2003b). There are only a few studies that reconstruct the fetal jaw in 3D from histological sections (Norberg, 1933; Radlanski, 2003b; Radlanski et al., 2016). Note that due to laborious nature of histological reconstructions only single specimens at representative ages were studied. Radlanski himself points out that it would be better to have a bigger 3D sample upon which to base descriptions of the tooth bone interface (Radlanski et al., 2016). The acquisition of human material showing sequential prenatal developmental stages is very rare and a unique opportunity to study sequential growth.

Non-destructive 3D imaging is now possible for mineralized and non-mineralized tissues. The advantage is that fetuses are intact so there is perfect registration of the virtual slices. The best techniques are in vitro μ CT imaging where ossifying bones can be reconstructed in 3D (Gondre-Lewis et al., 2015; Morimoto et al., 2008; Neumann et al., 1997; Reid et al., 2015). This μ CT does a far better job of imaging complex anatomy compared to 2D radiographs that project all the information from the Z axis onto one plane either occlusal-lingual (Van der Linden et al., 1972) or bucco-lingual. The recent paper by Radlanski (Radlanski et al., 2016) further highlights the variability in the septae between the dental crypts. We hypothesize that higher

throughput μ CT will permit general patterns of bone morphology to be determined since more specimens can be examined.

In our study we were fortunate enough to have acquired a unique sample of human fetuses from the middle trimester (12-19 weeks). We have employed the method of μ CT to image intact fetal heads and used sophisticated 3D analysis software to calculate volumes, linear dimensions and shape changes in the teeth over time.

1.3 Hypotheses

Hypothesis 1: μ CT will have sufficient resolution to determine bone changes surrounding the teeth during the middle trimester

Hypothesis 2: Growth of tooth crypts and the mandible are proportionate to the age of the fetus

Hypothesis 3: Tooth follicles are fully encased in bone and the bone dictates tooth morphology

Hypothesis 4: Teeth are not originally in individual crypts but as the fetus ages, septae appear between tooth morphotypes

Hypothesis 5: Morphogenesis of crowns is not regulated by the bone. Here I would expect to see tooth follicles developing without adjacent bone. The teeth would grow allometrically since they are free to change shape without the constraining influences of bone

1.4 Aims

1. To measure 3D growth morphogenesis of the mandible and alveolar bone during the fetal period
2. To visualize the tooth crypts within the alveolar bone using digital segmentation methods
3. To quantify growth of the tooth crypts as a proxy for follicle growth during the middle trimester. in 3D using morphometrics

4. To measure shape changes of tooth crypts using landmark-based geometric morphometrics

Chapter 2: Material and Methods

2.1 Origin of the specimens

Whole human fetal heads were obtained by Dr Diewert (Professor of Orthodontics at UBC) for a research project that was funded in the 1980's by the BC Foundation for Health Research. The fetuses were obtained as a result of spontaneous or elective terminations at BC Children's and Women's hospital carried out between 1986 and 1988. The conceptuses were stored in glass jars in 10% formalin solution. Each specimen was given a coded number by the hospital so no personal identifiers are available. The hospital also provided crown-rump length, head circumference and estimated days post conception. New approval to work on these specimens was obtained by the supervisor (Human ethics protocol H08-02576). For this study we selected fetuses from 12 to 19 weeks (middle trimester). Midweek dates were selected as close as possible for each sample. The samples were also selected ensuring that the days of gestation were close as possible within the age groups (Table 2.1). Three samples from each age group were identified fitting these criteria making a total of 25 samples. However, the 13 week age group had 4 samples of similar days post conception therefore, all four were used (Table 2.1).

Table 2.1 Characteristics of the fetuses used in the study

Coded Specimen numbers	Days p.c.	Sex	pontaneous elective	orCRL (mm)
12_1	89	F	E	99
12_2	85	M	E	90
12_3	?	?	E	?
13_1	?	?	E	?
13_2	96	M	E	112
13_3	91	M	E	102
13_4	91	?	?	?
14_1	103	?	?	?
14_2	104	M	E	127
14_3	103	M	E	125
15_1	109	F	E	137
15_2	108	F	E	135
15_3	108	M	E	135
15_4	107	M	E	133
16_1	115	F	E	149
16_2	114	M	E	146
16_3	116	M	E	149
17_1	122	F	E	159
17_2	123	M	E	161
17_3	124	F	E	164
18_1	128	F	E	166
18_2	128	M	E	166
18_3	128	F	E	166
19_1	133	F	E	170
19_2	133	M	E	170
19_3	137	M	E	181

Table. 2.1 The sample set used was provided by Dr. Diewert , (UBC, BC, Canada) . The sample set was collected at Women’s hospital, BC, Canada. It consists of 25 specimens ranging from 3-4 samples per age group. The days post conception, sex, and the mode of acquisition ie spontaneous or elective and the CRL were noted by the pathologist at the time of acquisition.

2.2 Micro computed tomography scanning

The samples were removed from the formalin solution and were rinsed in distilled water several times. The foetal heads were then placed in several ziplock bags to prevent fluid leakage. The wrapped foetal heads were placed in plastic holder tubes. The diameter of the specimen holder was 88 mm. The heads were scanned in the sagittal plane in a Scanco Medical uCT 100 (Brütisellen, Switzerland). The field of view (cross section) for the whole scan was 90.1 mm. The isotropic voxel size was 50 μ m. The scanner was set at 70kVp with a current of 200 μ A. The integration time was 500ms. The filter was 0.5mm Al. DICOM stacks were reconstructed into 3D using Amira software (v5.6, FEI, Oregon) to create isosurfaces. Segmentation of the mandible and tooth crypts was done in Amira. To separate the image of interest from the background the voxel values are used. Any voxel having a value lower than the assigned threshold is registered as 'exterior' and any voxel value greater than the assigned threshold is assigned as interior. Any artefacts can be suppressed by using the 'remove couch' option which will ensure only the most coherent area will be labelled. The threshold that I set was 1200. This threshold was arrived at after trying many different values. The same threshold was used to generate the isosurfaces..

2.3 Segmentation of the mandible and tooth crypts

The mandible was segmented along with individual tooth crypts using the segmentation tool on the Amira 5.6 software. The wand tool was used to automatically select contiguous pixels through the DICOM image stack that corresponded to the mandible (Fig. 2.1A,C,E). Since the mandible is an independent structure from the skull this automatic method was feasible. Segmenting the tooth crypts required manual segmentation. Each tooth crypt was identified by scrolling through the stack of slices. Here I varied the grey scale threshold to ensure that all bony features were captured. The paintbrush tool was used to colour in the space created in the

mandibular bone by the tooth crypts. This is done in the three directions: the sagittal, the coronal and the transverse orientation (Fig. 2.1B, D, F; sagittal and coronal views not shown). This enables a complete segmentation of each tooth crypt (i1, 12, c, m1, m2) from the right side (quadrant 8) and the left side (quadrant 7).

Figure 2.1 Segmentation method to mark the boundaries of the crypts within the mandibular bone

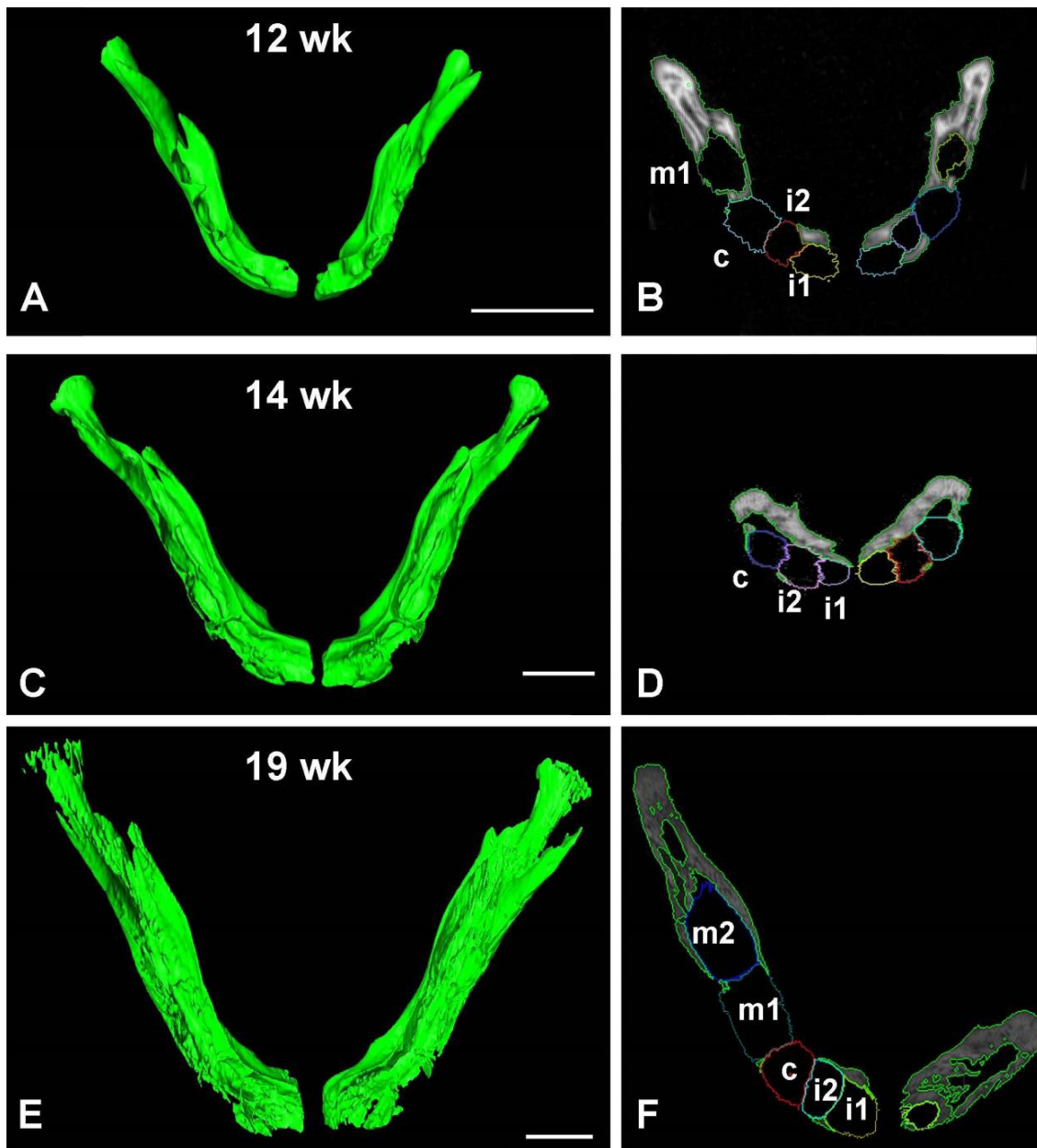


Fig. 2.1: Segmented mandibles in horizontal section at 12, 14 and 19 weeks. The wand tool is used to select contiguous pixels through the DICOM image stack and the resulting image is seen in A, C, E. The images seen in B, D and F are representative slices through

2.4 Measurements

Volumetric and linear measurements were carried out in the Amira program. The material statistics option automatically calculates volumes of the segmented portions. The linear dimensions were measured using the 3D measurement option on the Amira 5.6. The mesio-distal (MD), the bucco-lingual (BL) and the inciso-gingival (IG) measurements were approximated. This was made easier by being able to toggle off all the other crypts except the one that was being measured and moving the image in all directions. The various images can then be toggled back on for example the mandible to ensure correct orientation of the measurement (Figure 2.2A,B)

The segmentation was repeated independently three times for each canine crypt (73 and 83) on eight samples from 12 to 19 weeks gestation (one per week). The mean volumes of the re-segmented crypts were used to calculate the percentage intra-observer error. The buccal fenestration was also noted for each tooth of each sample. This was done by observing the buccal aspect of the segmented mandible of each sample of each age group. the fenestration was noted as being fully open, partially closed or closed. The observations were compiled into a table (Table 3.1, Appendix 1)

Figure 2.2 Location of measurement landmarks for standard morphometrics

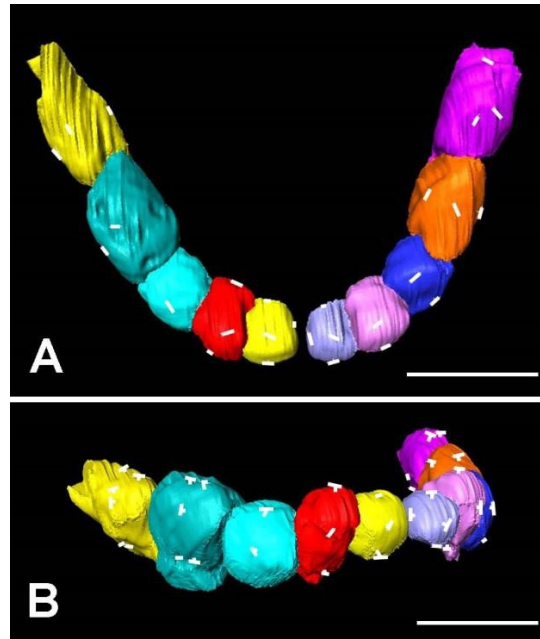


Fig. 2.2 Horizontal section (A is occlusal view and B is the R lateral view) of 19 week specimen tooth crypts with the mandible toggled off. The white marks represent the measurement marks.

The files of the segmented tooth follicles on Amira 5.6 were saved as PLY files to be able to be imported by the Landmark program. Landmark based morphometrics enabled me to analyze changes in shape of the tooth crypt and thus the tooth follicle within the middle trimester (Table 2.1). It was necessary to use an approach where the size changes are removed from the analysis so that instead we are measuring pure shape change. In order to carry out this analysis, I used landmark-based geometric morphometrics. I exported the segmented volumes as a mesh of triangulated points or ply files to Landmark software. The crypt surfaces were registered in space so when I applied landmarks to the surfaces, the software was able to record XYZ coordinates. Landmarks were selected based on homologous structures that could be recognized on all the teeth, the ability to place the landmark repeatedly on multiple teeth across multiple specimens and based on the minimum landmarks required to capture the form of each tooth (Table 2.2, Fig. 2.3) (Zelditch et al., 2012). Landmarking was carried out several times.

Figure 2.3 Homologous landmarks

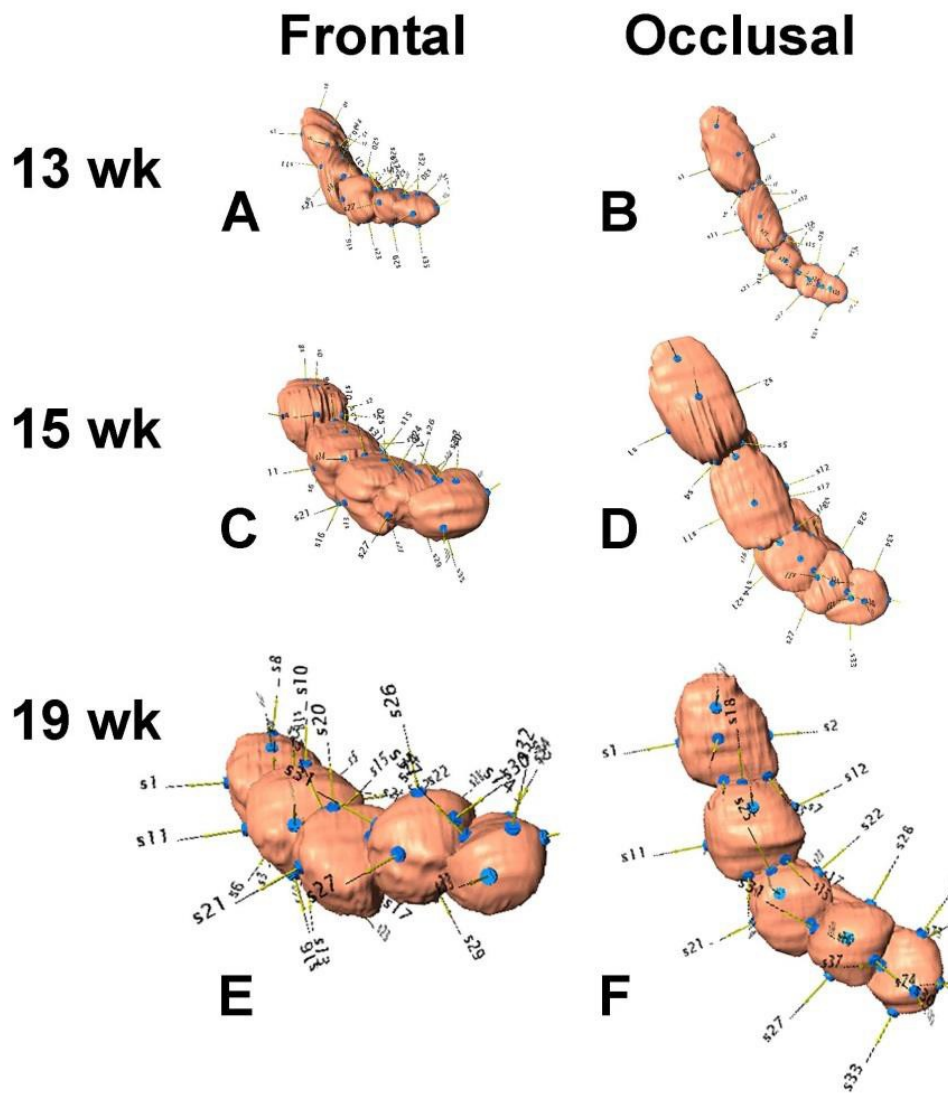


Fig. 2.3 10 landmarks for the molar teeth and chose 6 landmarks for the canine and the incisors were chosen according to Zelditch, (Zelditch et al., 2012). Zelditch's recommendations were to choose landmarks according to homology, adequate coverage of form, repeatability and consistency of relative position. See table 2.1 to identify landmark location.

Table 2.2 Location of homologous landmarks on tooth crypt volume renderings

Tooth number	Landmark number	Location on crypt
85	1	Incisal centre
	2	Buccal centre
	3	Lingual centre
	4	gingival centre
	5	mesial inciso buccal
	6	mesial inciso lingual
	7	mesial gingival buccal
	8	mesial gingival lingual
	9	Distal incisal
	10	Distal gingival
84	11	Incisal centre
	12	Buccal centre
	13	Lingual centre
	14	gingival centre
	15	mesial inciso buccal
	16	mesial inciso lingual
	17	mesial gingival buccal
	18	mesial gingival lingual
	19	Distal incisal
	20	Distal gingival
83	21	Incisal centre
	22	Buccal centre
	23	Lingual centre
	24	gingival centre
	25	Mesial incisal
	26	Distal incisal
82	27	Incisal centre
	28	Buccal centre
	29	Lingual centre
	30	gingival centre
	31	Mesial incisal
	32	Distal incisal
81	33	Incisal centre
	34	Buccal centre
	35	Lingual centre
	36	gingival centre
	37	Mesial incisal
	38	Distal incisal

2.5 The landmark based software Morpho J to analyse shape changes

The data points from Landmark were exported as X,Y,Z coordinates as a DTA file. The DTA files were imported into Morpho which connects the points to generate a simplified shape. The analysis starts with Procrustes Superimposition of all the shapes and average centroid size is determined. A new covariance matrix is then generated. Next principal component analysis is carried out (PCA) followed by canonical variate analysis (CVA). Discriminant Function Analysis (DFA) is carried out to compare the displacement of landmarks between specific data sets. To show the change in position of the landmarks between the two data sets 'lollipops' are created. The head of the lollipop shows the starting point and the tail shows the movement and the end point. Wireframes are created connecting all the landmarks for each tooth so that the shape of the tooth crypts is shown in relation to position changes of the landmarks between the 12 and 19 weeks. I did not repeat landmark-based geometric morphometrics on the same teeth to determine the variability in landmark placement.

2.6 Statistics analysis

The contralateral teeth were considered technical replicates for this study. The mean values for volume, BL, MD, IG length were taken for each tooth morphotype and these averages were used in subsequent analyses. Each specimen therefore provided data for 5 teeth, the central incisor (i1), lateral incisor (i2), canine (c), first primary molar (m1) and second primary molar (m2). Lower case letters indicate teeth are from the primary dentition. There were 3-4 biological replicates for each tooth at each week gestation. Descriptive statistics (averages and SD of volumes and linear measurements) were completed using Excel software (2013). Inferential statistics were done using Statistica

(v8.0, Statsoft Inc. Tulsa OK). The Shapiro Wilks test of normality was performed first for the mandibular volume and volumes of each of the teeth. Any cases where the p value was <0.05 meant there was significant skewing of the data (data was not normally distributed). One Way Analysis of Variance followed by Tukey's post-hoc test was used to see whether data for each week gestation was significantly different across the whole data set.

Chapter 3: Results

The μ CT scans were successful on all specimens, except one in which ossified tissue could not be detected. This specimen was discarded and replaced with a specimen that had appropriate ossification. In all specimens, the pathologist had removed the brains which led to collapse of the calvaria. Therefore head diameter and other measurements on the skull roof cannot be carried out to verify the original head measurements made when the samples were originally obtained. Several specimens did not have information about days post-conception, sex or crown-rump length. However due to the intact nature of the head, they were still included in the study. I tested several intensity thresholds in order to detect the thinnest wisps of bone but yet avoided artifacts. I chose a value that could be used across the samples that captured all the main features for the isosurfaces.

All of the intramembranous bones were present in the 12 week conceptuses and the ossified basi-occipital bone (Fig. 3.1A-A''). The mandible with the coronoid and condylar processes was also well differentiated however the symphysis was open (Fig. 3.1A-A''), Elsewhere in the face, the maxilla, zygoma, premaxilla and palatine bones have formed (Fig. 3.1A-A''). The orbital rim is incomplete at this stage. At 14 weeks the squamosal bone is more obvious as are the nasal bones. The maxillary bone and calvaria have expanded (Fig. 3.1B-B''). As the calvaria grow toward each other the sutures begin to form (Fig. 3.1C-D''). By 16 – 19 weeks the infraorbital and mental foraminae are visible. The enamel of the central incisors is sufficiently mineralized to appear at 16 weeks. The maxillary incisors are more advanced than mandibular incisors.

Figure 3.1 Isosurfaces of whole human fetal skulls from 12-19 weeks

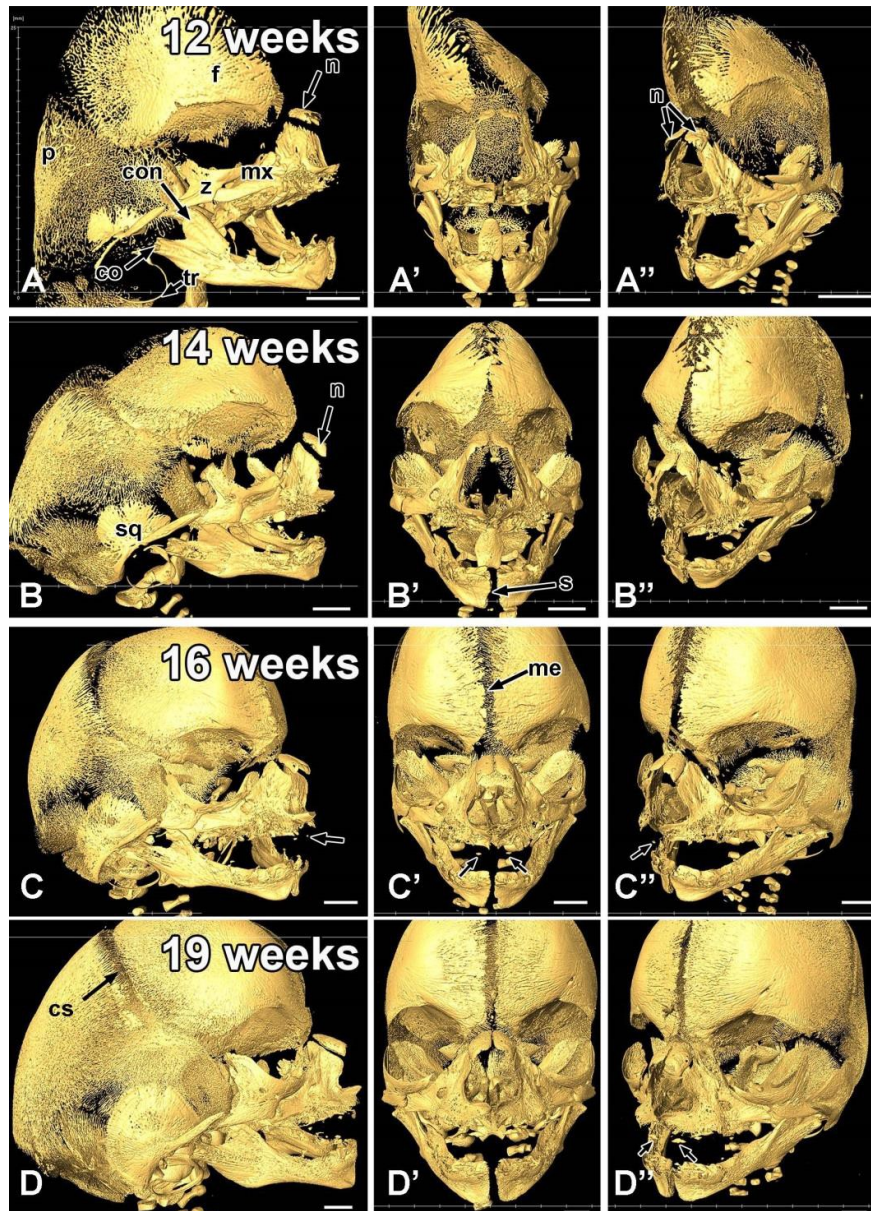


Fig 3.1 Images A to D show R lateral view, A' to D' in frontal view and A'' to D'' in Left lateral view. **A-A''**) At 12 weeks the parietal (p) and frontal (f) bones are visible, the calvaria are radiating out from the ossification centres. The mandible consists of condyle (con) and the coronoid (co) process. The maxilla (mx) is very thinly ossified in comparison to the zygoma (z). The zygomatic arch and the orbital rim are incomplete. The base of the skull is not formed but the basilar part of the occiput can be clearly seen through the open jaws (A'). The nasal (n) bones are present and the tympanic ring (tr) are visible. **B-B''**) At 14 weeks the gaps between the bones are decreased. The squamosal (sq) bone is more visible and the symphysis menti (s) is closing. **C-C''**) At 16 weeks the metopic sutures (me) have formed. The maxillary incisors are starting to mineralize (arrows). **D-D''**) At 19 weeks the zygomatic arch is more recognizable but still not articulating with the zygomatic process of the temporal bone or the zygomatic process of the maxilla. Mineralized incisors are visible (arrows in D''). Scale bars= 5 mm

3.1. Alveolar bone morphogenesis

Our sample of fetuses had encompassed the period when the body of the mandible had formed and bone was being induced by the tooth follicles. The primary dentition is undergoing morphogenesis, passing from cap to late bell stage. We anticipated that tooth crypts would be visible at 12 weeks but would be incompletely formed. We chose to study the mandibular dentition rather than the maxillary because the maxillary the bone is much thinner and the crypts would be less well-defined. The mandibular bone is highly ossified at 12 weeks so I could start the analysis of crypt morphogenesis in the youngest specimens in our sample. Had I studied maxillary crypt morphogenesis, I would be limited to the last few weeks of the sample available to me. Finally, the mandibular bone is separate from the rest of the skull which allows semi-automatic segmentation through the image stack. The maxillary bone has highly complex anatomy and is articulating with other bones. Segmentation of the maxillary bone according to the position of sutures would be impossible to carry out using the automated tools.

The semi-automatic segmentation of the mandible was successful in detecting very small features even in the youngest specimens. For segmentations, I varied the threshold as I moved through the slices in order to capture the thinnest, partially mineralized bone. This is different than creating isosurfaces where I kept the threshold at a standard value. The first observation was the follicles were not completely surrounded by bone. Certain trends were maintained for the entire 12-19 week period. There was no occlusal bone covering the enamel organs (Fig. 3.2A-E''). There were also very few inter proximal septae. This lack of inter proximal bone resulted in a common crypt for m1 and m2 as well as for i1 and i2. The first septum to form was between m1 and c (Fig. 3.2A,A''). At 13 weeks the septum between c and i2 initiated (Fig. 3.2B-B'') and became more robust in the older specimens (Fig. 3.2C-E''). There was lingual bone on all the specimens throughout the dentition. Gingival or basal bone

lining the bottom of the crypts was generally present, although there was a channel extending from m2 to c. This channel may represent a narrow opening in the bone. In contrast, the base of the i1 and i2 crypts had shallow, concave indentations which suggested the follicles were positioned superior to the bone. Finally, there was variable buccal bone along the dentition. It was difficult to determine from the mandibular segmentations whether the tooth follicles had induced bone on the buccal surface. Therefore it was necessary to identify the edges of the radiolucent follicle from serial slices.

Figure 3.2 Segmented mandibular bone reveals formation of the septae between crypts

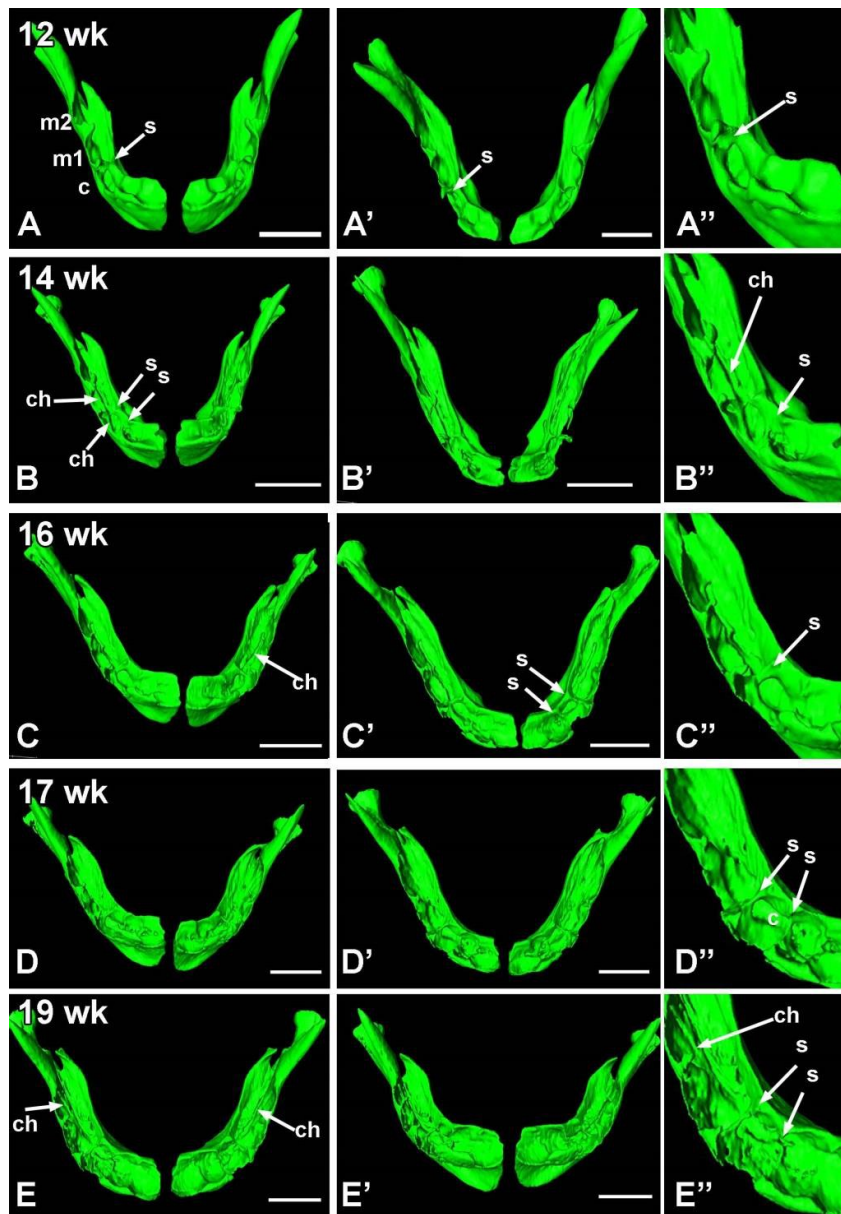


Fig. 3.2 Segmented images of the mandible from 12 to 19 weeks. The crypts of the i1, i2 are continuous as are m1 and m2. A-A'') At 12 weeks the only septae that are visible are distal to the crypt of the c (s). There is a channel which contains the mandibular nerve at the base of the m1, m1 and c crypts (ch). The i1 and i2 crypts are not separated and are very shallow. The m1 and m2 crypts are also continuous at their base but there is a bone spicule on the buccal side between the m1 and m2. B-B'') By 14 weeks the septum between c and i2 has developed. C-C'') At 16 weeks, the labial bone on i2 has increased where as i1 has a much shorter fringe of bone. D-D'', EE'') The septae on either side of the c are more advanced as is the channel in the bases of crypts m2, m1 and c. Scale bar = 2.5 mm for A,A' and 5 mm for the remaining panels

3.2. Buccal plate fenestration is highly variable in the mandibular dentition

After segmenting the teeth within the mandibular bone it became clear that buccal bone was absent in some regions of the dentition (Fig. 3.3A-E''). In contrast the lingual bone was complete in the entire sample. Tooth crypts were also mostly covered by bone on the gingival/basal surface but there was a small channel going from mesial to distal under the m1, m2. The c has a smaller channel compared to the molars and the incisors have no opening in the basal bone (Fig. 3.3E). The occlusal surfaces of the crypts were not covered by bone in any of the specimens. There was also a transient period where the primary incisors were forming above the dentary bone in 12 week specimens. We do not know whether other tooth crypts were above the bone at earlier stages however tooth morphogenesis is only in bud stage at this time so likely the bone is inferior to the teeth. The surprising changes in buccal bone integrity required further analysis.

3D analysis revealed fenestrations next to the buccal surfaces of teeth throughout the fetal period. The two areas with consistent buccal fenestrations are adjacent to the canine and first primary molar. The canine is wide open from 12-14 weeks (Table 3.1, Appendix 1), at 15 weeks 4/6 canine crypts have bone encroaching from the mesial and distal and 2/6 are fully exposed. Surprisingly at 16-18 weeks the majority of canines are fully open but at 19 weeks, bone begins to cover the mesial and distal corners of the crypt. In the first molar, the bony changes are even more variable. At 12 weeks 2/6 teeth are fully open on the buccal but then the majority of molars are fully open at 13 weeks. At 14 weeks the fenestra has partially closed on the majority of tooth crypts (5/6). The fenestra then is changing between mostly open to mostly closed between 15 and 16 weeks. Between 17 and 19 weeks the majority of m1 crypts have bone encroaching from the mesial and distal. There is a band of bone forming close

to the future site of the mental foramen (Fig. 3.3). We evaluated the presence of the mental foramen as well as details of the buccal bone spicules that partially cover the buccal surfaces of m1 and m2 on both the right and left sides of each specimen. There was a surprisingly high degree of symmetry (Table 3.1, Appendix 1). We did not include i1 and i2 in the symmetry analysis because these teeth are always symmetrical in terms of bone coverage on the buccal. For example, i1 follicle is always exposed on the buccal but i2 is almost always covered with bone. This may be due to the follicle forming above the bone for i1 as noted at 12 weeks. The i2 is also above the bone at 12 weeks but at 13 weeks the labial bone is creeping up the follicle (Fig. 3.3B,B'). The high degree of symmetry in the pattern of bone suggests that there is local patterning taking place but this is genetically controlled rather than environmentally regulated.

Table 3.1 Buccal Fenestration phenotype by specimen

Weeks gestation	Tooth type	Description of buccal bone			Symmetrical on R and L for c, m1 and m2
		Open fully	Partially closed	Closed	
12 weeks	i1	0	0	0	3/3
	i2	0	0	0	
	c	6	0	0	
	m1	2	4	0	
	m2	2	2	2	
13 weeks	i1	8	0	0	3/4
	i2	0	0	6	
	c	8	0	0	
	m1	6	2	0	
	m2	0	8	0	
14 weeks	i1	5	1	0	3/3
	i2	0	0	6	
	c	6	0	0	
	m1	1	5	0	
	m2	0	6	0	
15 weeks	i1	4	2	0	2/3
	i2	0	2	4	
	c	2	4	0	
	m1	2	4	0	
	m2	0	6	0	
16 weeks	i1	6	0	0	3/3
	i2	0	2	4	
	c	6	0	0	
	m1	4	2	0	
	m2	0	6	0	
17 weeks	i1	5	1	0	3/3
	i2	0	6	0	
	c	6	0	0	
	m1	0	6	0	
	m2	0	6	0	
18 weeks	i1	4	2	0	1/3
	i2	0	6	0	
	c	5	1	0	
	m1	3	3	0	
	m2	0	6	0	
19 weeks	i1	6	0	0	3/3
	i2	0	0	6	
	c	1	5	0	
	m1	0	6	0	
	m2	0	6	0	

Figure 3.3 Relationship between the buccal bone and the tooth crypts is highly variable

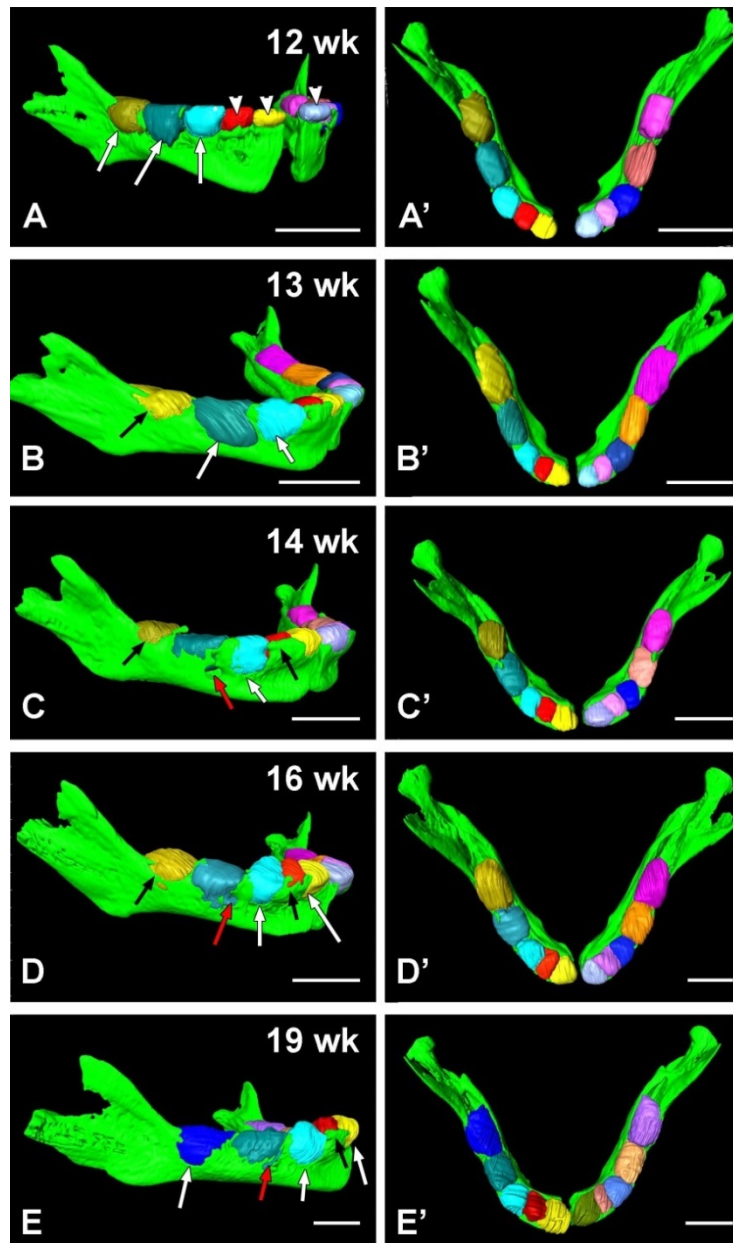


Fig. 3 Buccal bone appearance. A-A) Buccal bone is absent on m2,m1 and c (white arrows). i1 and i2 are above the bone (arrowheads). B-B'') bone is encroaching from the gingival margin on m2 (black arrow). The m1 and c are open on the buccal but the i2 is now covered with bone. C,C') Bone is covering half of m2 (black arrow) and a band of bone is crossing m1 forming the mental foramen (red arrow). The c has bone encroaching from the mesial and distal but the central thirds still exposed (white arrow). The i1 is fully exposed on the buccal. D.,D') Buccal surfaces of m1 and m1 are largely exposed except for a thin band (black arrow m2) and spicules of bone on m1 (red arrow). The c is exposed on buccal (white arrow) but there bone covering i2 (black arrow). Now the i1 has opened up more (white arrow). E,E') The m2 is fully exposed on the buccal (white arrow). The mental foramen is forming on the mesial buccal gingival corner of m1 (red arrow). The c and i1 are open on the buccal surface (white arrows).

3.3. Quantification of mandibular volume and variability in the sample

Once automatic segmentation of the mandible was carried out we could perform an initial unbiased assessment of the variability in our sample. For example, were there any outliers? I had selected specimens to cluster as closely as possible to post conception days for each week gestation. However it was possible that there was variation between fetuses. I could not use crown rump length since this was not available for all the specimens. Others prefer to use crown-rump length especially if they have the whole fetus in the anatomical collection. I only had heads. Head circumference could have been used however again this information was not consistently collected. It was not possible to measure head circumference on the samples since by the time they were sent to the lab the brains had been removed. As mentioned above, this lack of internal tissue greatly distorted the calvaria.

The increase in volume of the mandible is a good indicator for the growth of the mandible. The increase in CRL between 12 to 19 weeks indicates the growth of the fetus. This appears to be different to the growth of the mandible. The fetal growth appears to be linear and the mandibular growth appears to be in a step wise manner. Indeed after carrying out ANOVA and Tukeys post-hoc testing I found there to be three groupings 12-14 weeks, 15-16 weeks and 17-19 weeks. The 15-16 weeks were significantly different to the 12-14 weeks and the 17-19 weeks were significantly different to the 15-16 weeks. Thus the mandible appears to go through growth spurts as opposed to the CRL.. Generally the specimens clustered tightly within each age for the CRL (Fig. 3.4). When there appears to be 2 points such as for 12, 16 and 18 weeks, two of the three specimens overlap in volume. The most spread in specimen size is seen at 17 weeks where one specimen is nearly 25% larger than the smallest one in the group. In addition this large specimen is as large as the largest 19 week specimen. It is also surprising that the three, 18 week specimens were smaller than some of the 17 week specimens. In fact the

smallest 18-week specimen was almost as small as the largest 15 week. We attribute the variation to actual differences in body size between fetuses and not due to fetal demise. All the specimens analyzed in our study were elective terminations rather than spontaneous. We assume these terminations were carried out at the request of the mother, independent of genetic diagnoses or for medical reasons. We could not exclude any fetuses from our study based on health of the mother since this information was not available. Thus variation between 17-19 week specimens would probably result in not detecting size differences using statistical analysis.

Figure 3.4 Distribution of specimens by week gestation, mandibular volume and CRL

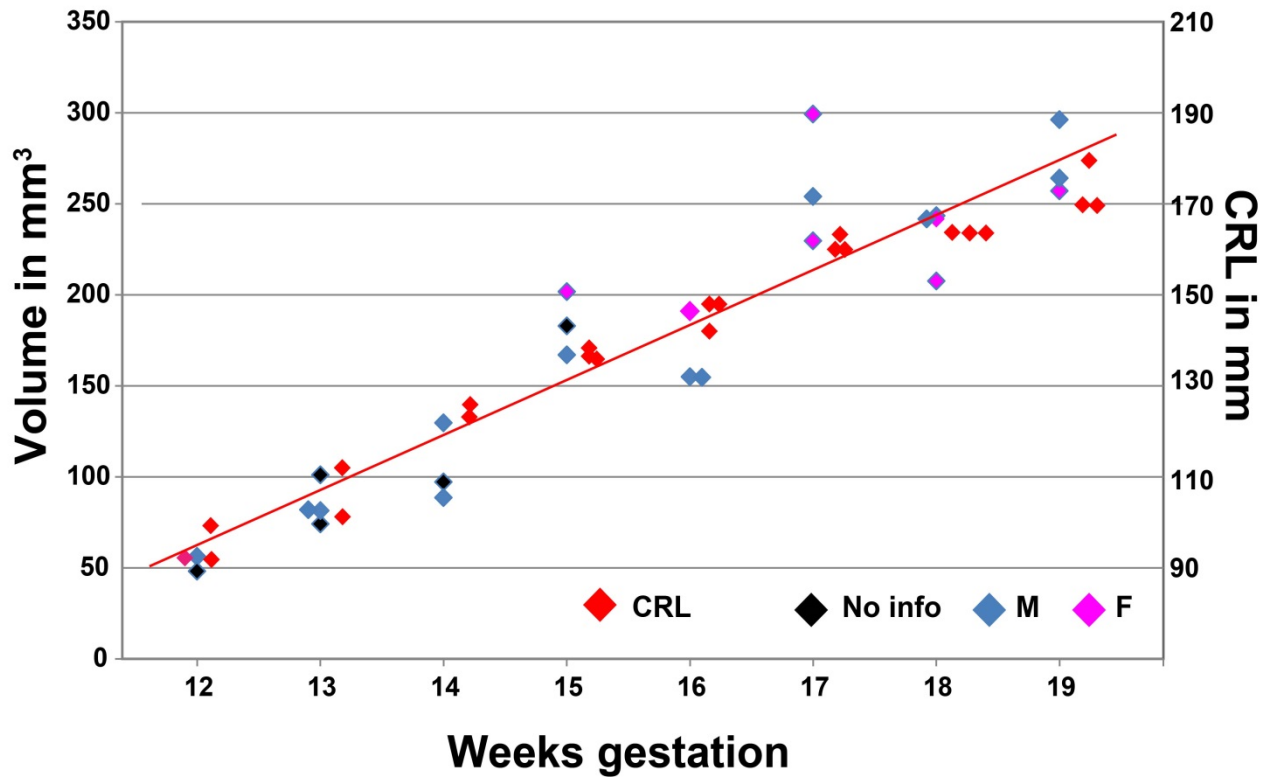


Fig. 3.4 The increase in CRL is linear whereas the increase in the mandibular volume is in a step wise manner. Conceptuses clustered close together in each of the weeks for the CRL demonstrating that the samples chosen were very close in somatic growth. No outliers were seen based on CRL In mandibular volume there was a female outlier at 17 weeks that was larger than the largest 19 week specimen. The other two 17 week specimens were male and were smaller than this one outlier. This demonstrates that biological sex is not a major determinant of mandibular size. Furthermore, mandibular growth is under different controls than somatic growth.

Before carrying out statistical analysis, it was important to know if the data is normally distributed or not so we know whether to do parametric or non-parametric analysis on the data. Normality was tested using the Shapiro-Wilks test. The Shapiro-Wilks test showed that if all of the mandibular volumes were entered, the data is normally distributed ($p = 0.1$ therefore we reject the hypothesis that the data is skewed). The numbers of observations for the different size ranges were normally distributed (Figure 3.5). When we look at the tooth and mandible volumes, some teeth were not normally distributed including the i1 and m1. The i2, c, m2 and mandible were normally distributed. For simplicity we carried out ANOVA analysis on all the segmented volumes, regardless of normality. There are three reasons for data skewing. 1) the sample size is too small 2) the segmentations are inconsistent 3) or there are more specimens that are on the larger end of the spectrum than the smaller end due to extensive growth in this period. I investigated the reproducibility of tooth segmentations by re-segmenting the canine three times on one specimen from each week gestation. The reasoning was that the canine almost always lacks a buccal plate and was technically difficult to define on the slice views. The results showed that the majority of canine resegmented volumes were within 5% of the mean value (Table 3.2). Thus reproducibility is good and does not explain the lack of normality in the incisors and m1

Figure 3.5 Shapiro-Wilks test of normality

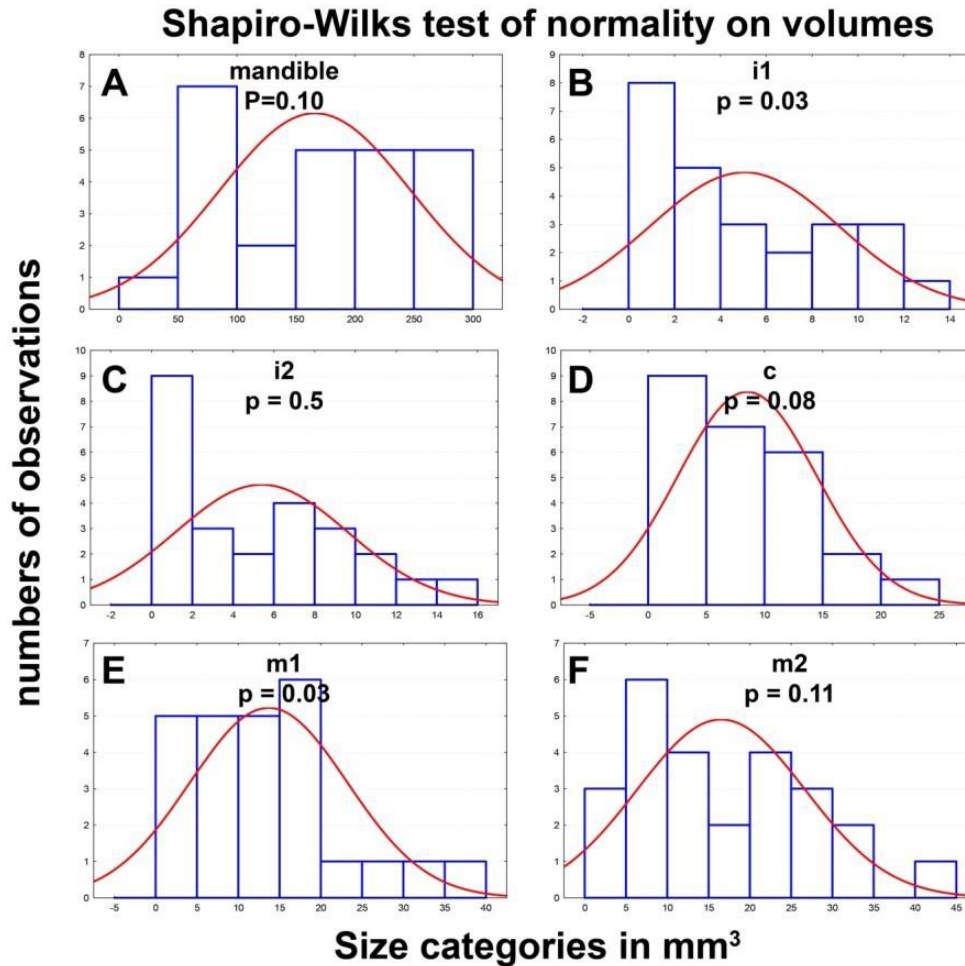


Fig. 3.5 Graphs showing the Shapiro-Wilks test of normality. When p is above 0.05 then we reject the hypothesis that the data is skewed. In other words a p value of greater than 0.05 means the data is normally distributed. The mandible, i2, c and m2 were normally distributed and the i1 and the m1 were skewed.

The growth of the mandible was clearly not linear and occurred in a punctuated fashion (Fig. 3.4). The analysis showed that for mandibular volumes the 12, 13, 14 weeks were not statistically significant from one another. The specimens 15 and 16 weeks were not statistically significant from one another and the 17, 18 and 19 weeks could also be grouped as another group. Each group was statistically significantly different than the other two. This ANOVA analysis matched closely the scatter plot in which overlap between specimens was clearly seen between 12-14 weeks, 15-16 weeks and 17-19 weeks (Compare Fig. 3.4 to 3.6A). We could therefore combine specimens within these groups if desired.

Table 3.2 Reproducibility of segmentation as shown by repeated measurements of canine crypts

Specimen	Tooth number	Volume for each attempt	Averages of replicates	SD of replicates	Variance as percentage of average value
12-3	73	1.29	1.31	0.03	2.45
	73	1.35			
	73	1.30			
	83	1.47	1.45	0.04	2.57
	83	1.41			
	83	1.48			
13-1	73	1.25	1.24	0.05	4.15
	73	1.28			
	73	1.18			
	83	1.16	1.22	0.05	4.22
	83	1.23			
	83	1.26			
14-1	73	3.61	3.62	0.03	0.73
	73	3.65			
	73	3.60			
	83	3.52	3.91	0.34	8.71
	83	4.06			
	83	4.15			
15-3	73	7.60	7.32	0.24	3.27
	73	7.19			
	73	7.18			
	83	7.27	7.28	0.02	0.24
	83	7.30			
	83	7.27			
16-3	73	6.92	6.96	0.33	4.69
	73	7.30			
	73	6.65			
	83	7.02	6.98	0.34	4.90
	83	6.62			
	83	7.30			
17-1	73	10.78	10.63	0.37	3.50
	73	10.21			
	73	10.91			
	83	10.39	10.99	0.63	5.70
	83	11.64			
	83	10.95			
18-3	73	14.03	13.75	0.28	2.00
	73	13.48			
	73	13.73			
	83	11.95	14.91	3.67	24.65
	83	19.02			
	83	13.75			
19-3	73	15.70	14.26	1.24	8.72
	73	13.56			
	73	13.53			
	83	17.10	16.66	0.70	4.20
	83	15.85			
	83	17.02			

3.4. Tooth crypt volume

The individual tooth crypts were segmented which allowed volumetric and linear measurements. The right and the left sides were considered technical replicates and the average of the 2 crypts was used in further analysis. The biological replicates consisted of the average values for the specimens within an age group. After carrying out ANOVA and post-hoc testing the fetal tooth crypts fell into groups. Representative comparisons are illustrated (Fig. 3.6 B-F). For the i1, there was no significant difference between week 12 and week 15 or between 17 and 19 weeks, however there was a significant difference between these two periods (Fig. 3.6B). The i2 had a similar pattern although the 15-16 week group was not significantly different than the 12-14 or 17-19 week (Fig. 3.6C). This suggests that there is gradual growth of the i2 rather than in spurts. The general trend for c, m1 and m2 is that the last 3 weeks are significantly different from the first 3 weeks (Fig. 3.6D-F)

The large quantitative difference in volume seen for all the teeth crypts between 12 weeks to 17-19 weeks is reasonable because this is when morphogenesis is underway. Thus the segmentations of the inner edges of the crypts are assumed to be a fair representation of the growth of the follicle. The central incisor i1 has the greatest increase at 1794% increase from the 12 weeks to the 19 weeks. The second molar m2 has the least amount of increase at 564% increase. Interestingly this increase is a similar percentage of increase as the mandibular volume (Table 3.4). Thus the increase in crypt volumes gradually decreases as we move posteriorly in the mandible which may be due to the fact that more of the initial size of the follicle for the molars is specified at the start of fetal development.

Figure 3.6 Volumetric measurements

Volumetric increases during the middle trimester

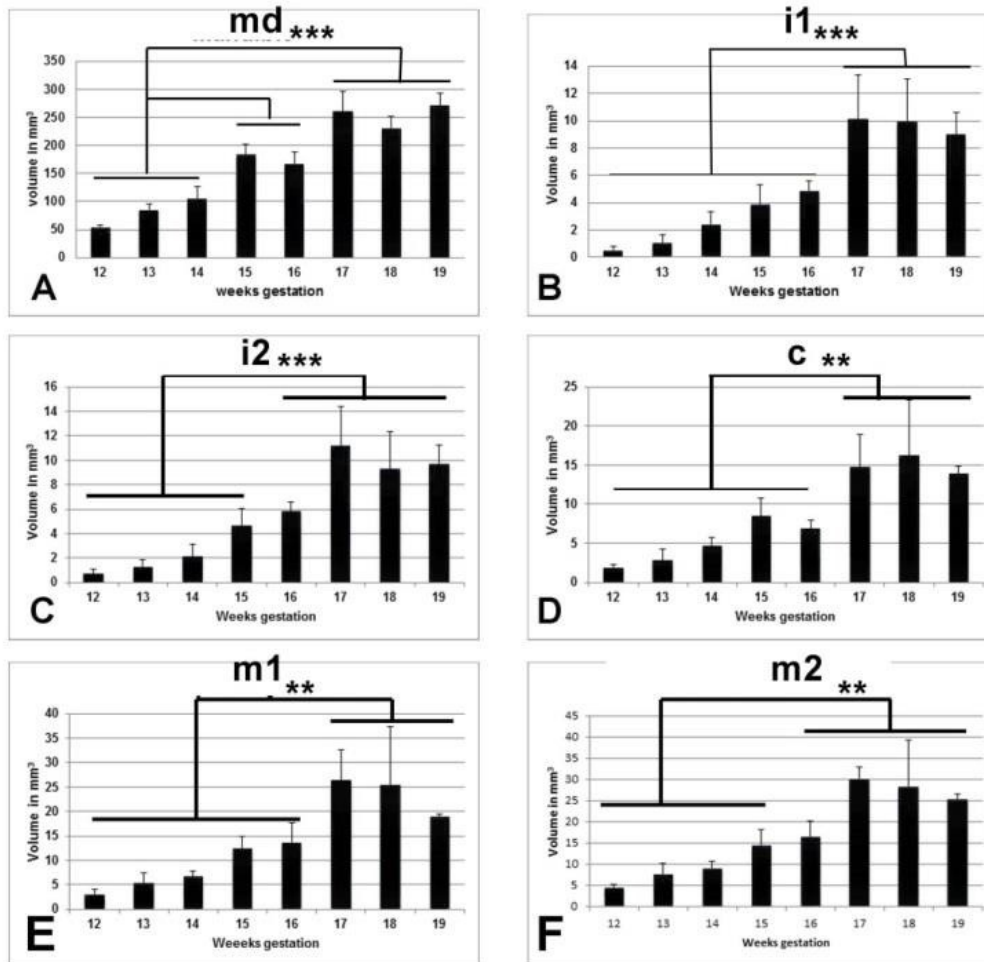


Fig. 3.6 The increase in crypt volumes is different to the increase in mandibular volume. The increase in volume of the crypts is not in the step wise pattern as the mandible. There is a gradual increase between 12 and 16 weeks, then there is a statistically significant increase at 17 weeks. * = $p < 0.05$; ** = $p < 0.01$; *** = $p < 0.001$

3.5. Tooth crypt dimensions

The overarching result was that there are natural groupings of data as determined by ANOVA and post-hoc testing such that 12-14 weeks and 17-19 weeks are significantly different (Fig. 3.7, 3.8, 3.9). The inciso-gingival and bucco-lingual dimensions had the most significant changes (Table 3.3). For example the IG length of i1 was significantly different between 12 weeks and 15 weeks ($p = 0.04$) and when compared to 16 weeks ($P = 0.02$). However when comparing i1 IG length between 12 and 17-19 weeks, the p values are 2 orders of magnitude smaller (p value range = 0.001 to 0.0008). Interestingly at 16 weeks the mean IG lengths for canine, m1 and m2 are smaller than at 15 weeks (Fig. 3.7C-E). The ANOVA analysis shows that there is no significant difference in IG length between the 12-14 week specimens and the 16 week specimens for m1 and m2. It appears that the crypts are contracting in this dimension possibly due to increased bone apposition on the basal surface.

The BL dimensions were similarly were significantly different between the 12-14 week and 15-19 weeks for all the teeth (Fig. 3.8A-E). The only slight exception is for m2 which is not significantly different between 12 and 15 weeks (Table 3.3). For the remaining teeth, the p values were generally lower than for the IG length (values range between 0.01 for m1 at 15 weeks to 0.0002 for m2 at 19 weeks, Table 3.3). In contrast to IG and BL, the p values for MD dimensions were larger (Fig. 3.9A-E). There were typically no significant differences between 12-16 week MD lengths. This is in contrast to the IG and BL measurements where 12-14 week values were often significantly different than 15-19 weeks.

Table 3.3 ANOVA and Tukey's Post-Hoc testing of IG and BL dimensions

Inciso-gingival

Bucco-lingual

A

Tukey HSD test, variable i1IG (Spreadsheet3)									
Approximate Probabilities for Post Hoc Tests									
Error: Between MS = .15259, df = 17.000									
Cell No.	weeks	(1)	(2)	(3)	(4)	(5)	(6)	(7)	(8)
1	12	68533	99750	1.2300	1.8167	1.9300	2.4600	2.5000	2.3267
2	13	0.958437	0.958437	0.679340	0.039885	0.019839	0.000831	0.000678	0.001728
3	14	0.679340	0.992137	0.992137	0.174597	0.089531	0.002786	0.002160	0.006672
4	15	0.039885	0.174597	0.604766	0.604766	0.400737	0.022004	0.017159	0.049780
5	16	0.019839	0.089531	0.400737	0.999950	0.999950	0.499476	0.428729	0.744969
6	17	0.000831	0.002786	0.022004	0.499476	0.709652	0.709652	0.636030	0.907803
7	18	0.000678	0.002160	0.017159	0.428729	0.636030	1.000000	1.000000	0.999173
8	19	0.001728	0.006672	0.049780	0.744969	0.907803	0.999851	0.999173	1.000000

F

Tukey HSD test, variable i1BL (Spreadsheet3)									
Approximate Probabilities for Post Hoc Tests									
Error: Between MS = .04336, df = 17.000									
Cell No.	weeks	(1)	(2)	(3)	(4)	(5)	(6)	(7)	(8)
1	12	1.0633	1.2175	1.5433	1.9200	2.0600	2.5100	2.5467	2.6100
2	13	0.973059	0.973059	0.153050	0.002149	0.000531	0.000168	0.000168	0.000168
3	14	0.153050	0.481182	0.481182	0.481182	0.007192	0.001324	0.000170	0.000169
4	15	0.002149	0.007192	0.389869	0.389869	0.104770	0.000689	0.000503	0.000327
5	16	0.000531	0.001324	0.104770	0.989163	0.989163	0.046826	0.030786	0.014735
6	17	0.000168	0.000170	0.000689	0.046826	0.205456	0.205456	0.143068	0.073140
7	18	0.000168	0.000169	0.000503	0.030786	0.143068	0.999998	0.999998	0.999311
8	19	0.000168	0.000168	0.000327	0.014735	0.073140	0.998622	0.999931	1.000000

B

Tukey HSD test, variable i2IG (Spreadsheet3)									
Approximate Probabilities for Post Hoc Tests									
Error: Between MS = .05952, df = 17.000									
Cell No.	weeks	(1)	(2)	(3)	(4)	(5)	(6)	(7)	(8)
1	12	95333	1.2100	1.3533	2.0800	2.4033	2.6833	2.8733	2.8633
2	13	0.855298	0.855298	0.504671	0.000721	0.000185	0.000168	0.000167	0.000167
3	14	0.504671	0.992715	0.992715	0.043070	0.000291	0.000172	0.000168	0.000168
4	15	0.000721	0.043070	0.033160	0.033160	0.001389	0.000242	0.000175	0.000176
5	16	0.000185	0.000291	0.001389	0.731496	0.731496	0.106691	0.017129	0.018923
6	17	0.000168	0.000172	0.000242	0.106691	0.842830	0.842830	0.319350	0.342962
7	18	0.000167	0.000168	0.000175	0.017129	0.319350	0.975306	0.975306	0.981639
8	19	0.000167	0.000168	0.000176	0.018923	0.342962	0.981639	1.000000	1.000000

G

Tukey HSD test, variable i2BL (Spreadsheet3)									
Approximate Probabilities for Post Hoc Tests									
Error: Between MS = .04957, df = 17.000									
Cell No.	weeks	(1)	(2)	(3)	(4)	(5)	(6)	(7)	(8)
1	12	1.2100	1.3525	1.7033	2.0667	2.1857	2.7467	2.5433	2.6667
2	13	0.988014	0.988014	0.184100	0.004015	0.001160	0.000168	0.000183	0.000171
3	14	0.184100	0.473005	0.473005	0.011102	0.002767	0.000169	0.000205	0.000174
4	15	0.004015	0.011102	0.510145	0.510145	0.201501	0.000635	0.004805	0.001320
5	16	0.001160	0.002767	0.201501	0.997137	0.997137	0.027648	0.213817	0.064890
6	17	0.000168	0.000169	0.000635	0.027648	0.097181	0.097181	0.531654	0.207590
7	18	0.000183	0.000205	0.004805	0.213817	0.531654	0.943739	0.943739	0.999791
8	19	0.000171	0.000174	0.001320	0.064890	0.207590	0.999791	0.996612	1.000000

C

Tukey HSD test, variable C IG (Spreadsheet3)									
Approximate Probabilities for Post Hoc Tests									
Error: Between MS = .06919, df = 17.000									
Cell No.	weeks	(1)	(2)	(3)	(4)	(5)	(6)	(7)	(8)
1	12	1.3433	1.6375	1.9133	2.8000	2.3600	3.2433	3.0067	3.0433
2	13	0.815125	0.815125	0.202854	0.000229	0.003843	0.000168	0.000173	0.000171
3	14	0.202854	0.857086	0.857086	0.000591	0.036609	0.000171	0.000226	0.000205
4	15	0.000229	0.000591	0.012790	0.012790	0.463332	0.000354	0.001944	0.001410
5	16	0.003843	0.036609	0.463332	0.480951	0.480951	0.472109	0.974071	0.940004
6	17	0.000168	0.000171	0.000354	0.472109	0.013191	0.110015	0.080623	0.080623
7	18	0.000173	0.000226	0.001944	0.974071	0.110015	0.947672	0.947672	0.978297
8	19	0.000171	0.000205	0.001410	0.940004	0.080623	0.978297	1.000000	1.000000

H

Tukey HSD test, variable C BL (Spreadsheet3)									
Approximate Probabilities for Post Hoc Tests									
Error: Between MS = .04103, df = 17.000									
Cell No.	weeks	(1)	(2)	(3)	(4)	(5)	(6)	(7)	(8)
1	12	1.2900	1.3750	1.8167	2.1667	2.0833	2.8900	2.6933	2.7900
2	13	0.999113	0.999113	0.080360	0.001318	0.003410	0.000167	0.000168	0.000168
3	14	0.080360	0.144997	0.144997	0.001853	0.005227	0.000167	0.000168	0.000168
4	15	0.001318	0.001853	0.443172	0.443172	0.737592	0.000273	0.001318	0.000615
5	16	0.003410	0.005227	0.737592	0.999492	0.999492	0.007849	0.080360	0.026161
6	17	0.000167	0.000167	0.000273	0.007849	0.002920	0.002920	0.924488	0.998350
7	18	0.000168	0.000168	0.001318	0.080360	0.030655	0.924488	0.924488	0.998684
8	19	0.000168	0.000168	0.000515	0.026161	0.009598	0.998350	0.998684	1.000000

D

Tukey HSD test, variable m1 IG (Spreadsheet3)									
Approximate Probabilities for Post Hoc Tests									
Error: Between MS = .10179, df = 17.000									
Cell No.	weeks	(1)	(2)	(3)	(4)	(5)	(6)	(7)	(8)
1	12	1.5583	1.8150	2.0700	2.5783	2.0750	3.5350	3.6883	3.0350
2	13	0.958378	0.958378	0.530388	0.019571	0.519108	0.000176	0.000170	0.000707
3	14	0.530388	0.959743	0.959743	0.088384	0.955554	0.000202	0.000174	0.002282
4	15	0.019571	0.088384	0.537941	0.537941	1.000000	0.000763	0.000347	0.029693
5	16	0.519108	0.955554	1.000000	0.549316	0.549316	0.031614	0.009825	0.656304
6	17	0.000176	0.000202	0.000763	0.031614	0.000787	0.000787	0.000354	0.030831
7	18	0.000170	0.000174	0.000347	0.009825	0.000354	0.998615	0.556924	0.255888
8	19	0.000707	0.002282	0.029693	0.656304	0.030831	0.556924	0.255888	1.000000

I

Tukey HSD test, variable m1 BL (Spreadsheet3)									
Approximate Probabilities for Post Hoc Tests									
Error: Between MS = .06584, df = 17.000									
Cell No.	weeks	(1)	(2)	(3)	(4)	(5)	(6)	(7)	(8)
1	12	1.4667	1.6650	1.9217	2.3400	2.5500	3.2017	3.1000	2.8933
2	13	0.980917	0.980917	0.465597	0.014313	0.002005	0.000170	0.000174	0.000235
3	14	0.465597	0.883135	0.883135	0.049225	0.005915	0.000172	0.000183	0.000321
4	15	0.014313	0.049225	0.511297	0.511297	0.112546	0.000388	0.000763	0.004435
5	16	0.002005	0.005915	0.112546	0.967831	0.967831	0.013224	0.034515	0.199498
6	17	0.000170	0.000172	0.000388	0.013224	0.092040	0.092040	0.212778	0.709139
7	18	0.000174	0.000183	0.000763	0.034515	0.212778	0.999603	0.999603	0.822338
8	19	0.000235	0.000321	0.004435	0.199498	0.709139	0.822338	0.974065	1.000000

E

Tukey HSD test, variable m2 IG (Spreadsheet3)									
Approximate Probabilities for Post Hoc Tests									
Error: Between MS = .08525, df = 17.000									
Cell No.	weeks	(1)	(2)	(3)	(4)	(5)	(6)	(7)	(8)
1	12	1.6200	1.8100	2.2183	2.5483	2.3833	3.3683	3.5450	2.9833
2	13	0.986816	0.986816	0.255147	0.020419	0.077767	0.000183	0.000170	0.000959
3	14	0.255147	0.609704	0.609704	0.063437	0.231938	0.000206	0.000173	0.001413
4	15	0.020419	0.063437	0.852343	0.852343	0.996158	0.003234	0.000638	0.078766
5	16	0.077767	0.231938	0.996158	0.996158	0.996158	0.049653	0.011533	0.613542
6	17	0.000183	0.000206	0.003234	0.049653	0.012731	0.012731	0.002944	0.252411
7	18	0.000170	0.000173	0.000638	0.011533	0.002944	0.994168	0.736094	0.320932
8	19	0.000655	0.001413	0.078766	0.613542	0.252411	0.736094	0.320932	1.000000

J

Tukey HSD test, variable m2 BL (Spreadsheet3)									
Approximate Probabilities for Post Hoc Tests									
Error: Between MS = .06620, df = 17.000									
Cell No.	weeks	(1)	(2)	(3)	(4)	(5)	(6)	(7)	(8)
1	12	1.5417	1.8250	2.0700	2.2817	2.5333	3.0550	2.8750	2.9367
2	13	0.826097	0.826097	0.253176	0.050855	0.003953	0.000168	0.000306	0.000247
3	14	0.253176	0.906040	0.906040	0.386465	0.036096	0.000332	0.012222	0.000720
4	15	0.003953	0.036096	0.906040	0.906040	0.395078	0.004206	0.023099	0.012895
5	16	0.050855	0.386465	0.906040	0.906040	0.889419	0.025774	0.129551	0.076191
6	17	0.000168	0.000332	0.004206	0.036096	0.039507	0.889419	0.265798	0.556616
7	18	0.000306	0.000332	0.004206	0.025774	0.265798	0.999603	0.999603	0.998959
8	19	0.000247	0.000720	0.012895	0.076191	0.556616	0.998959	0.999986	1.000000

To simplify the analysis I calculated the percentage change in the dimensions comparing the mean 12 week to mean 19 week values. (Table 3.4). The i1 dimensions were nearly identical at 17-19 weeks (2.5 mm) in the IG dimension but at 12-14 weeks the BL and MD were similar and the IG dimension was much shorter. The i2 was similar in all dimensions in the first 3 weeks but was proportionately narrower in the MD dimension compared to the BL and IG in the last three weeks. The c was fairly conical in the early period with a slightly narrower MD aspect. In the later period the c was longer in the IG diameter and shortest in the MD aspect. The m1 was much larger in the MD diameter at the early time point with the other two dimensions being equal. At 17-19 weeks there nearly a doubling in the BL and IG dimension and a relatively smaller increase in the MD dimension. Now however, the IG and MD diameters were equal, so there was a maintenance of the MD length with a concomitant increase in the IG length. The m2 maintained its proportions going from the early to later period with the smallest to largest dimensions being BL, IG and MD respectively. The molars therefore had a rectangular shape right from the start. Another trend that was observed was the increase in incisogingival length for the incisors and canine. This suggests that alveolar bone is growing more rapidly in the anterior part of the mandible. In contrast there is no single tooth that is responsible for increasing arch length (length of the dental follicles in the MD dimension) between 12 and 19 weeks. All teeth contribute equally.

Figure 3.7 Incisogingival length changes between 12 and 19 weeks

Inciso-gingival length

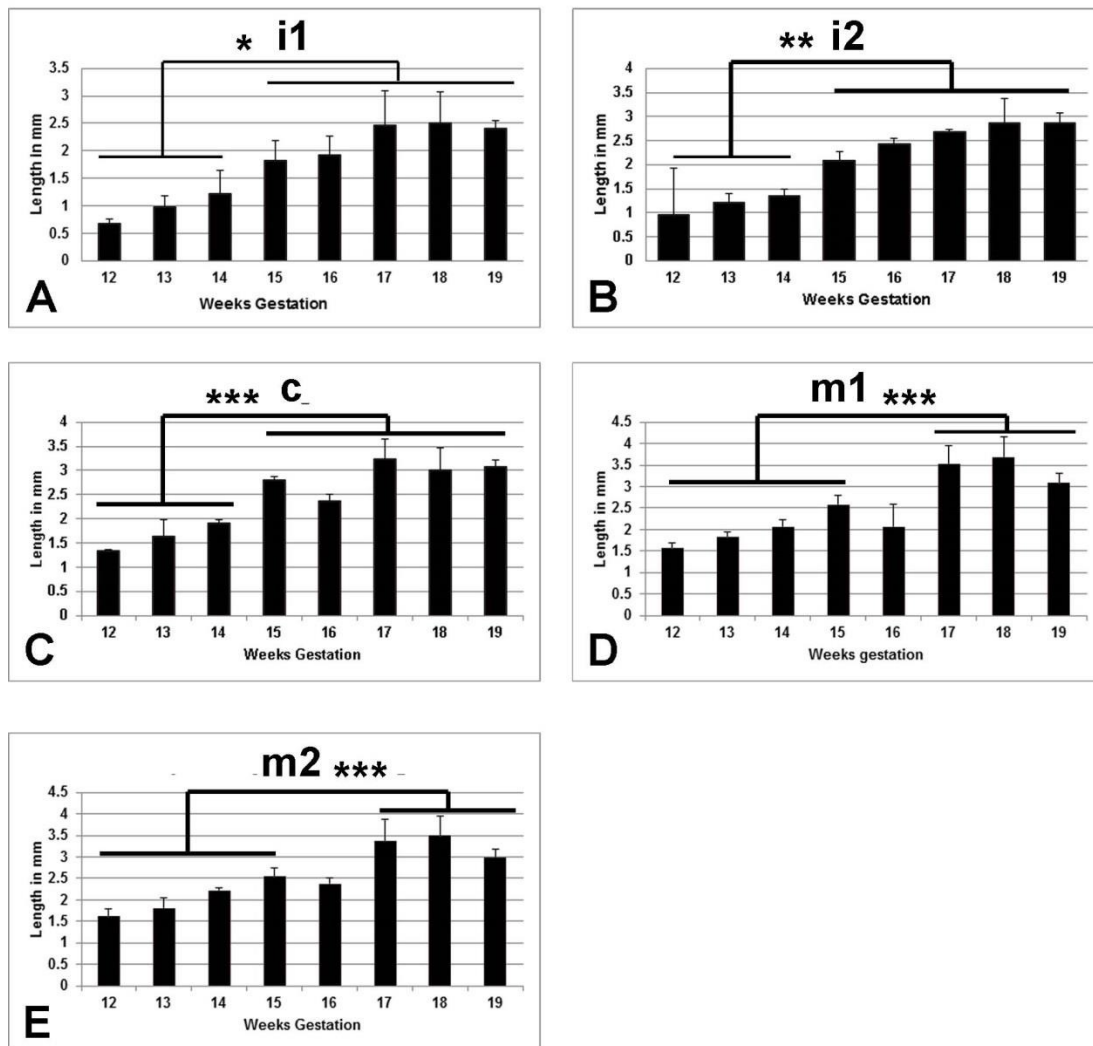


Fig. 3.7 The i1 and i2 and c show a significant increase in IG length between 12-14 and 17-19 weeks. The m1 nearly doubles in length. * = $p < 0.05$; ** = $p < 0.01$; *** = $p < 0.001$

Figure 3.8 Buccolingual length changes between 12 and 19 weeks

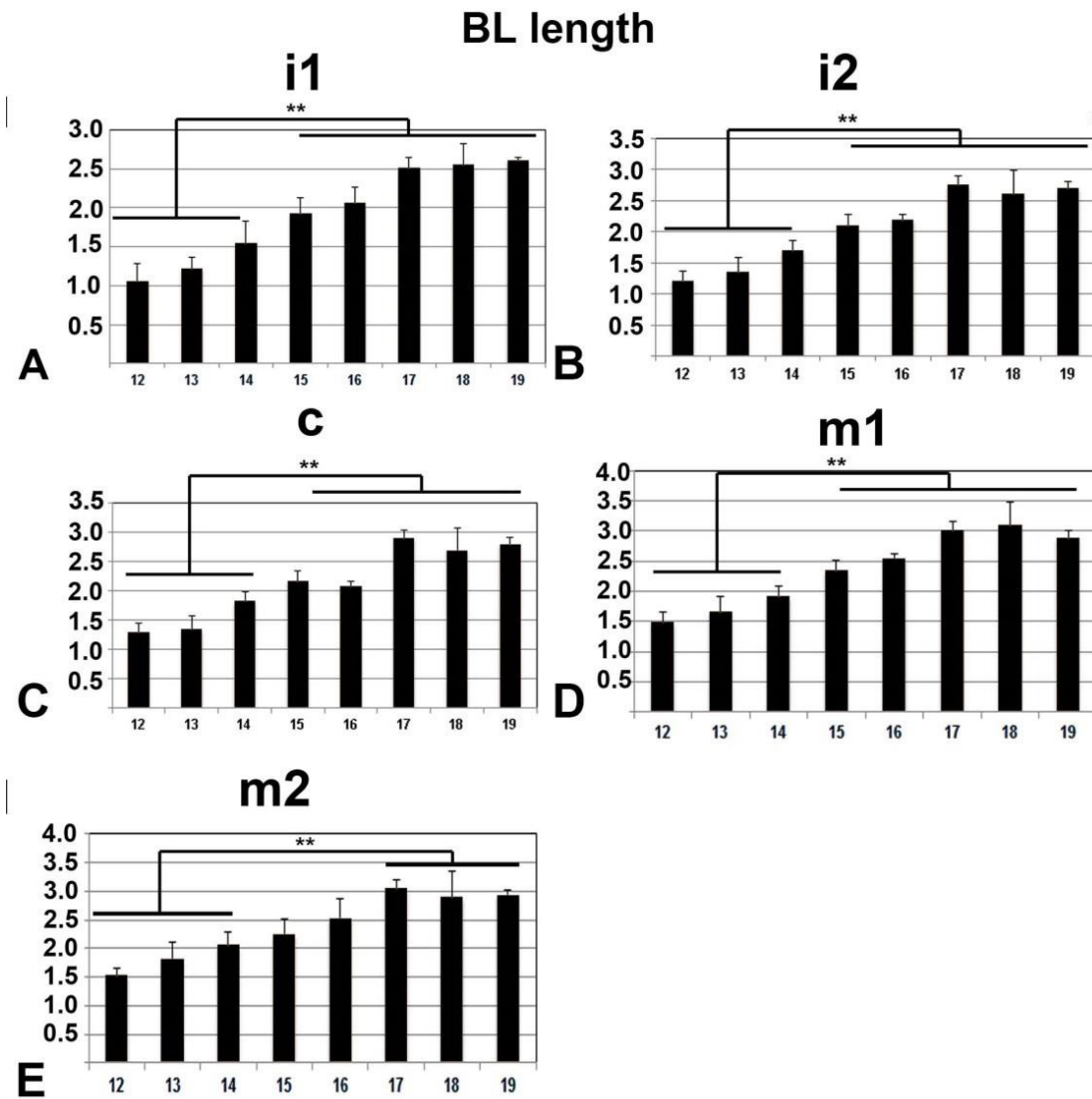


Fig. 3.8 In the bucco-lingual all teeth grow significantly when comparing the 12-14 week specimens to the 17-19 week. The m1 nearly doubles in size. The increased BL dimension at 17-19 weeks correlates with the induction of the successional teeth which must fit within the same crypt as the primary teeth . ** = $p < 0.01$.

Figure 3.9 Mesiodistal length

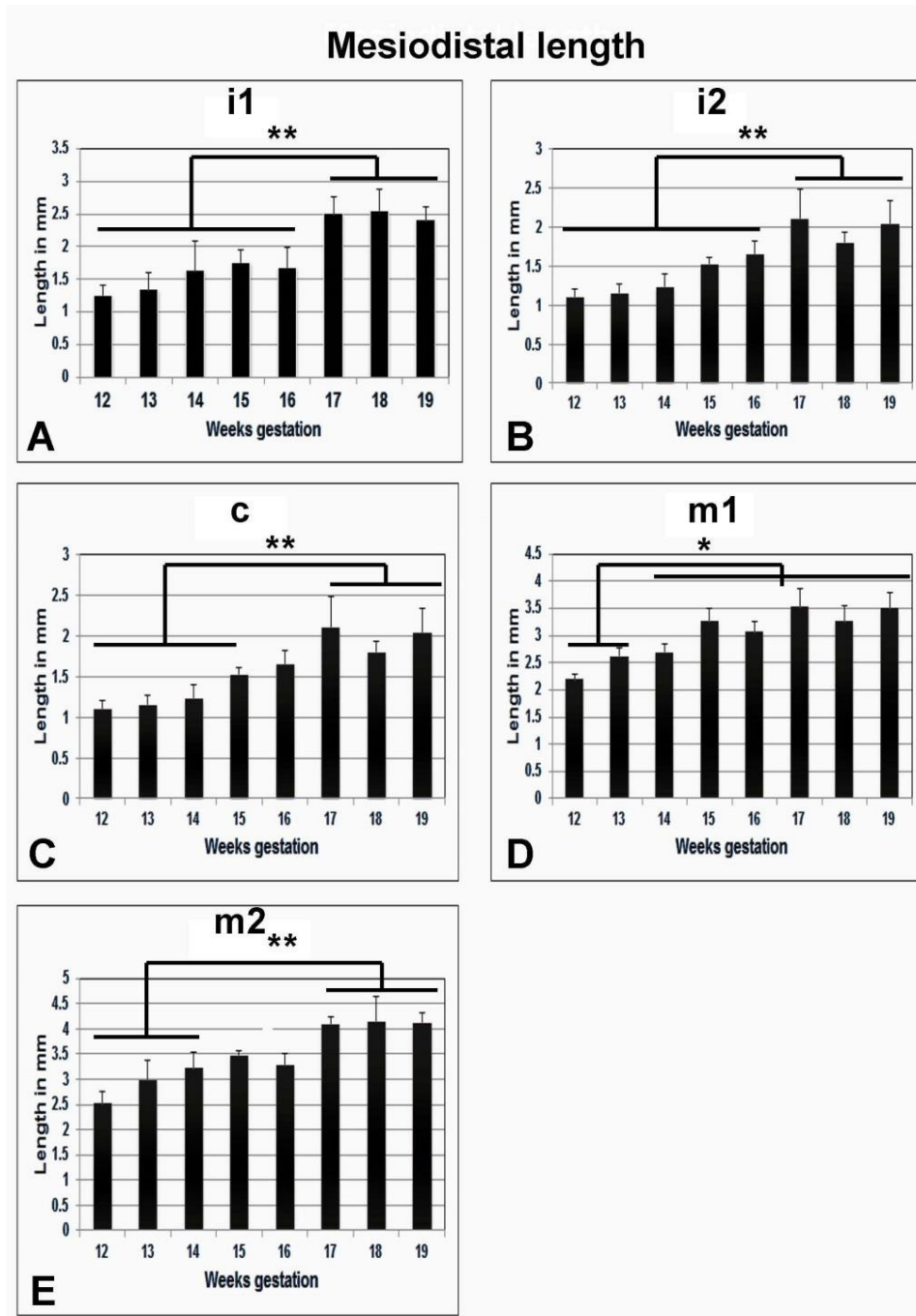


Fig. 3.9 In the mesio-distal dimension the i1, i2, c had the greatest increase whereas m1 and m2 experienced less growth. The m1 increases 1.4 fold whereas the m2 increases 1.3 fold.* =. $p < 0.05$; ** = $p < 0.01$

Table 3.4 Percentage increase in volume and dimensions between the average 12 week and average 19 week specimens

Structure	Percentage increase volume	Percentage increase MD length	Percentage increase IG length	Percentage increase BL length
Mandible	512%			
i 1	1794%	179%	352%	246%
i 2	1307%	164%	302%	223%
c	736%	169%	230%	216%
m1	620%	159%	197%	193%
m2	564%	163%	185%	190%

3.6 Morphometrics

Morphometrics analysis begins with Procrustes superimposition which translates, rotates and resizes shapes to find the mean shape. The first analysis is principal component analysis which involves finding the major sources of variation in the entire dataset. This is an unbiased way to find out whether shape of the dental crypts is different or whether all the data points are similar. All 5 teeth from the lower right quadrant were included for each specimen. Only the right side was included because the growth of the head in this time period would cause shifting of the sample and thus alter the landmarks if both left and right side were included. The software is not informed of the fetal stage. PCA analysis showed that there was one variable that explained most of the variation (Fig. 3.10). The PCA confidence intervals were useful for revealing outliers. The smaller circles indicated that more similar shapes were found in these groups. The confidence intervals with the largest spread were 14 weeks and 17 weeks. We had already identified an outlier in the 17 week group based on mandibular size however the 14 week shape distribution was different than the volumetric data. This difference could be real variation in shape or perhaps inconsistent landmark application.

Wireframes provide a visual representation of the landmarks and their deformation in 3D space (Fig. 3.11). What is very interesting is that the c and m1 have the most displacement in the buccal landmarks (Fig. 3.11A) where no buccal bone exists. Thus it appears the tooth can expand in the buccal direction. The i1, i2 and c are changing shape primarily by gingival and distal displacement of the crypt (Fig. 3.11B). This correlates with the increase in IG length. There is minimal shape change in the MD or IG landmarks for m1 (Fig. 3.11A,B). For m2, there is minimal buccal or lingual displacement of landmarks (Fig. 3.11A) however the distal aspect of m2 is greatly shifted towards the mesial direction as

seen in the occlusal (Fig. 3.11A) and buccal views (Fig. 3.11B). This compression of m2 may be due to the advancing development of M1 which I could see within the same crypt as m2.

Figure 3.10 Principal component analysis

Principal component analysis showing shape clustering by weeks gestation

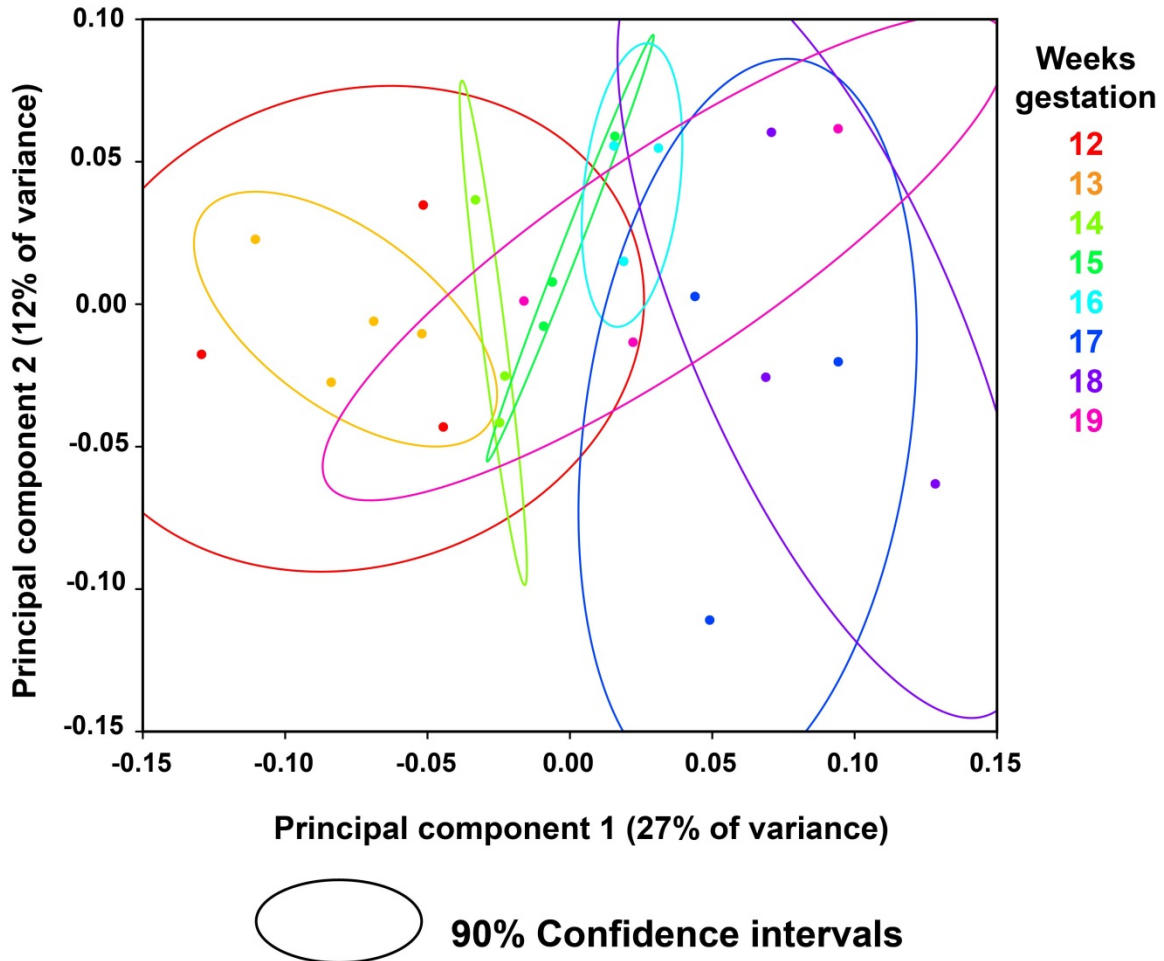


Fig. 3.10 PCA analysis of all 5 teeth as a unit. The units on the X and Y axes are arbitrary. The more similar in shape the samples are, the closer the data is clustered to the 0:0 point. The major variation in 12 and 13 week data is along the X axis whereas most of the variation in 19 and 18 weeks was in the Y axis. The confidence intervals overlap considerably between 12 and 13 weeks showing that shapes are similar. There are also major overlaps between 15 and 16 weeks. The outliers appear to be in the 17 week and 18 week groups.

Figure 3.11 Discriminant function analysis with wireframe graphical output showing shape changes

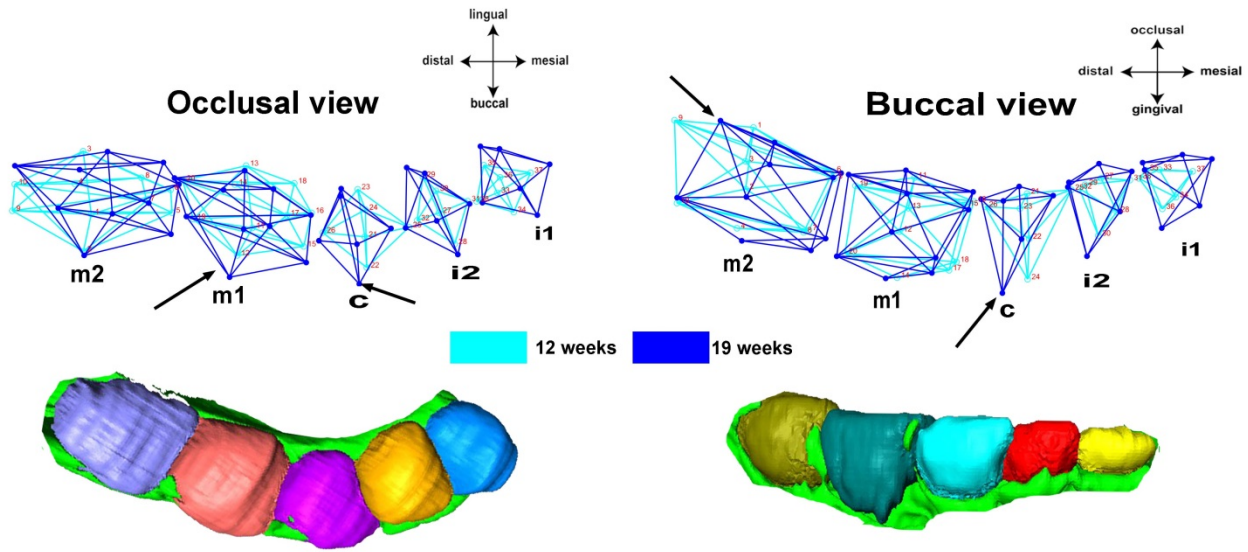


Fig. 3.11 A comparison of the mean shapes from 12 week and 19 week specimens from the occlusal and buccal views using Discriminant Function Analysis. Landmarks are represented by dots. Representative segmentations are shown below the wireframes. **A)** The wire frameworks show that the i1, i2 and c show buccal displacement of the buccal landmarks (black arrows). There is also lingual displacement of the lingual landmarks for c, i2 and i1, possibly to accommodate the forming successional teeth. Interestingly, there is no lingual displacement of landmarks for m1 and m2, perhaps because successional teeth have not yet initiated. **B)** In the buccal view, there is displacement of the gingival landmarks towards the distal especially for the c (black arrow). The m2 had mesial displacement of the distal landmarks (black arrow) which could be due to expansion of the crypt to include M1. The m2 occlusal landmarks have been displaced towards the mesial at 19 weeks which may coincide with the onset of mineralization of the cusps.

Chapter 4: Discussion

4.1 Micro-CT imaging reveals temporal and spatial changes in fenestration of the buccal bone, and septation between crypts

In my study I discovered that the alveolar bone was constantly changing in the extent of coverage of the tooth crypts. The lingual surface was present throughout, the gingival concavity was mostly intact except for a channel running mesio-distally, the occlusal surface was never covered and the most surprising result was that buccal bone was highly variable. The most consistent fenestration in the buccal bone was on the canines and the m1. The c was always exposed on the buccal surface, whereas m1 often had bands of bone spanning the buccal side. There were few interproximal septae between the teeth, except for the mesial and distal of the c. These findings agree and extend the work of others that looked at human dental and alveolar bone development (Kjaer and Bagheri, 1999; Ooë, 1981; Radlanski et al., 2016). One previous study focused specifically on the incisors and canines (Kjaer and Bagheri, 1999). These authors looked at 16-19 week fetuses using histology and several skeletonized preparations from 18-21 week fetuses. In all cases, buccal bone was not present on the maxillary and mandibular canines (Kjaer and Bagheri, 1999). In this study it was proposed that the canines may be moving buccally and thus preventing bone from forming. However in my study there was never a time where buccal bone was present next to the canine. It seems unlikely that pressure can explain the lack of bone, especially when one considers that the teeth are in early bud stage in 12 week fetuses.

I determined that there was a specific correlation between the presence of buccal bone on the m1 and the mental nerve that was not previously reported. Indeed, the likely reason for bone forming in on the mesial side of m1 was to enclose the mental nerve. A detailed analysis of the mental nerve revealed that foramen was fully formed by 17 weeks but prior to that time, there was

more variability between fetuses. Interestingly, the development of the mental nerve was synchronized on the right and left sides suggesting that temporal regulation of development is genetically controlled. The close relationship of the buccal bone on m1 and the mental nerve implies that factors being released by the nerve are positive signals for bone induction. I did not examine the maxilla so it would be interesting to know whether the same pattern exists without the presence of a major nerve on the buccal side of m1. There is some data on the maxillary m1 in a study by Kjaer (Kjaer and Bagheri, 1999). Although they did not comment on the m1, the sections pass through this tooth in several illustrations. It appears that in the maxilla there is buccal bone on m1, although the position of the bone relative to the occlusal surface is not known. More work using microCT reconstructions will help to resolve this question.

Radlanski recently described the presence of buccal fenestra on the c and m1 in the mandible using computer-aided reconstructions of fetal sections (10-28 weeks) (Radlanski et al., 2016). The detail obtained from histological sections was superior to what one could see with μ CT, this is because the usual section thickness is between 7 -10 μ m, whereas in μ CT the voxel size was $50\mu\text{m}^3$. Therefore, the histological sections were 5 times more detailed. Nevertheless, there is surprising concurrence of the data. Radlanski described that the lingual plate is fully covering the tooth crypts and that there is a basal opening in the bone inferior to the follicles for the mandibular nerve (Radlanski et al., 2016). Radlanski also documented resorption and apposition of bone in the walls of the crypts by counting osteoclasts (TRAP staining) or osteoblasts (mononuclear cells on the bone surface). He

proposed that the follicle was constantly interacting with the bone, causing resorption of the inner surface of the crypt. A similar pattern of increased numbers of osteoclasts lining the developing crypt was observed in the mouse (Alfaqeeh et al., 2013). However unlike Radlanski who presented images of fetuses that were 10, 11, 12, 14, 17, 22 and 28 weeks gestation, I have presented data on 25 fetuses using tables and images from different specimens. Radlanski only studied the right mandible in specimens older than 11 weeks. I analyzed right and left sides using the averages of crypt sizes for each tooth type. Also I compared the patterns of bone deposition on the right and left sides and determined there was a striking degree of symmetry. Thus my work is relatively larger in scope which has revealed some trends that are difficult to discern in the more focused type of study.

Taken together, it is interesting that teeth can undergo morphogenesis with or without being completely enclosed by a bony crypt. The basal resorption of the crypt as noted by Radlanski (Radlanski et al., 2016) correlates with the deformation in shape between 12 and 19 weeks that we observed for the incisors and canines. Here the gingival landmarks were shifted further gingivally for all three teeth but less so for the molars. The dimensional changes in IG length correlate with resorption of the inner surfaces of the crypt however the tooth germs were also expanding in an incisal direction due to expansion of the enamel organ (increased volume of the stellate reticulum to support amelogenesis). I could not directly visualize the follicles but based on the height of the bone extensions, there was clearly also incisal growth. An indication of the weakness in my methodology was that for some stages, dimensions of the crypt appeared to decrease compared to the previous week. Here the likely explanation is that there is increased bone apposition on the inner surface of the crypt which may shorten the IG length. In addition there could be variability

in the segmentation of the crypts in these specimens. Nevertheless, segmented tooth crypt volumes did capture the main features of tooth morphogenesis during the fetal period as shown by others in histological reconstructions but to be certain that the whole follicle is identified, contrast agents must be used to visualize the non-mineralized tissue directly.

4.1.1 Interactions between adjacent tooth follicles

One of the most interesting findings was the lack of septae between m1, m2 and between the incisors. Our data shows that the canine was the only tooth with septae on mesial and distal sides and even then the bone was not very dense. The lack of separation of the incisors and molars means that contact between the follicles is direct. Although not segmented in my study, there is also no septum between m1 and m2. There may be contact inhibition mechanisms that prevent expansion of the follicles. Evidence for one follicle having a dominant role over the shape of the adjacent follicle is seen with m2. Our shape analysis shows that instead of expansion of all the landmarks between week 12 and 19 for m2, there is an unexpected compression of distal landmarks so that they are displaced mesially. This is exactly the kind of evidence that would support a hypothesis that tooth germs influence the shape of neighbouring teeth. The m2 is a particularly interesting case because the m1 is so much larger and is forming on the distal surface of m2.

4.1.2 Growth of tooth crypts is proportionate to mandibular growth but not linear

Volumetric and linear distance measurements carried out on the tooth crypts and mandible show a clear relationship. This makes sense when one considers that there must be room created in the mandible in order to fit the enlarging teeth. Radlanski documented apposition of bone on the outer surfaces of the mandible which increases space for the crypts (Radlanski et al., 2016). The greatest increases in growth in our study were in the inciso-gingival dimension.

Similarly, the greatest displacement of landmarks in the morphometric analysis was towards the gingival. Thus I presume there must be a concomitant increase in the height of the body of the mandible. Radlanski reported that by 24 weeks there was considerable apposition of bone to the crest of the alveolus (Radlanski et al., 2016). Due to the quantitation that I was able to carry out using segmented volumes I have more insights into the rate of mandibular and crypts growth over time. I found that the first 3 weeks of our study (12-14 weeks), there was little size increase for most of the measurements but by 17-19 weeks there was a very significant growth spurt such that the increase in mandibular volume is over 500%. A similar spike in growth was observed by Ooë (Ooë, 1981). He measured mandibular tooth diameters from histological reconstructions from 3 months to birth. In this case, he traced the dental epithelium of the tooth germ rather than measuring the mineralized parts of the tooth which would not be present in the younger conceptuses. There was little increase in MD and BL diameter of the incisors and canines between 12-16 weeks. There after there was a sharp increase in size, leveling off by 7 months. The incisors had reached their final size by 7 months but the canines continue to grow until birth. Even though my measurements were made on the negative space within the mandibular bone that contains the tooth follicles, I was able to confirm and to extend the data of Ooë. Unlike in his study, I could more precisely determine which teeth grew incrementally (the c, m2) and which grew in a punctuated manner (i1, i2, m1). Moreover I could measure diameter of the segmented crypts in all 3 dimensions which provided new insights into the IG growth parameters. Ooë also did not study the molars. Therefore the methods I have developed are able to cover a larger data set in more detail.

4.2 Is the mandibular bone controlling the shape of the follicle or vice versa?

Many tooth development researchers suggest that the follicle induces the bone and thus the bone follows the morphogenesis of the tooth. However a paper carried out on mouse molars has taken new approach to this question (Alfaqeeh et al., 2013) . Teeth were explanted with and without mandibular bone and their growth and proliferation was followed in organ culture. The teeth cultured without bone grew larger and this was due to increased proliferation (Alfaqeeh et al., 2013). The caveat with this study is that it is hard to prevent tissues from spreading out in organ culture. This happens to all cultures whether or not they were originally surrounded by bone. However the increased proliferation is very intriguing and suggests that bone has a negative effect, perhaps by secreting inhibitory cytokines. Most tooth organ cultures in tooth development studies are carried out without the bone present (Balic and Thesleff, 2015; Thesleff, 2014) so perhaps we are not seeing the true shape develop as it would in vivo.

My work suggests that we cannot extrapolate from mouse to human. The fact that mice do not form successional teeth means that the crypts surrounding mouse molars are different than those surrounding the primary human dentition. The successional teeth (incisors, canines, premolars) form lingual to the primary teeth and are initiating at 17 weeks (Ooë, 1981; Radlanski et al., 2016). These secondary teeth are therefore contained within the crypts that I segmented in the 17-19 week specimens. Many studies document the fact that permanent premolars have not formed by the end of the middle trimester (Logan and Kronfeld, 1933; Ooë, 1981; Radlanski et al., 2016). Indeed the premolars are in early bell stage after birth (Ooë, 1981). The presence of successional teeth does appear to affect the shape of the crypt and by extension the follicles for c, i2 and i1. In my study there were

displacements of buccal and lingual landmarks for only these three teeth. When studying the mouse crypt it is more analogous to that of the human permanent molars which are only forming at birth. Our fetal study cannot be replicated in the mouse model. It is likely that the bone-tooth interactions taking place during fetal development set up fields of developmental interactions that persist postnatally. The lack of septae between i1 and i2 provide necessary space for the larger permanent incisors to undergo morphogenesis. The similarity in shapes of the incisors may relate to the close proximity of the follicles. It seems that it is just as important to repress bone formation in certain locations as it is to induce bone. In other words, the requirement for the bone to shape the crown seems low during morphogenesis stages. However, when the roots form, it is essential for bone to be closely connected in timing and position to the extending cervical loops. In this way induction of the periodontal attachment can take place.

4.3 Limitations of the study

Segmentation of the tooth crypts is reliant on the observer's interpretation of the radiopaque, mineralized tissues. In some cases bone may be partially ossified, so that the x-rays do not detect the matrix. Contrast agents can dramatically improve staining of soft tissue as well as partially mineralized bone (Fig. 4.1A-E'). A particular weakness in my crypt segmentations is the delineation of the occlusal surface which is not covered by bone. I assumed that the highest extension of the interproximal bone represented the highest point on the occlusal surface. Subsequent studies have verified this assumption using PTA staining (Fig. 4.1E,E'). The distal surface of m2 was also hard to determine since there was no distal septum. Further studies in which the PTA stained specimens are segmented will verify my data on crypt development during the fetal period.

Another limitation of my study is that the landmark based morphometrics was not repeated several times. The placement of the landmarks may not be consistent on certain surfaces especially the distal of m2 because this surface was hard to segment. If I were to repeat this study I would look carefully through the segmentations and repeat those which were outliers. The I would reapply landmarks several times to check the reliability.

A limitation of my study was the small sample size to perform Geometric Morphometrics analysis, particularly canonical variant analysis and discriminant function analysis. For landmark based GM we would need to calculate our sample size based on a total of 38 landmarks. According the Zelditch's calculation (Zelditch et al., 2012) ($N = 3 \times \text{number of landmarks} - 7$) we would need 107 specimens. Alternatively we would need to dramatically decrease the number of landmarks to 1.5 which is not feasible. One idea is to take each tooth separately and analyze it. Then we would have 3×10 (landmarks for molars) -7 or a minimum sample size of 23. We are within the acceptable range. To further increase sample size we could use the left side teeth, flip them horizontally thus doubling the sample size. This new approach could be taken with the existing dataset.

Another limitation of landmark-based geometric morphometrics is that the major axes of variation are mathematically determined. It is hard to interpret the morphometric changes represented by PC1, PC2 etc. A different approach using Euclidean distance mapping of a specific specimen to a generalized average specimen for the group is a great alternative to PCA. A visual representation of the deformation of the surface is shown using a heat map (red is more prominent, blue is more depressed)(Kristensen et al., 2008). EDMA is more intuitive than PCA but the extent of changes is harder to quantify.

4.4 Future directions

4.4.1 Standard μ CT does not document the soft tissues

The studies from Ooe and Radlanski have the advantage of capturing the non-mineralized tissues and cellular details (Ooë, 1981; Radlanski et al., 2016) . The disadvantage is the incredible amount of labour required to align and trace the sections. These two individuals, Ooë and Radlanski have devoted their entire careers to the tracing and reconstruction of histological sections. The analysis of human data is very important because animal models do not represent all characteristics of humans. Humans have a much longer fetal period during which bone and soft tissues are molded. As reported by Radlanski, the mouse dentition mainly forms above the bone and then by birth is completely surrounded by bone (Radlanski et al., 2015; Radlanski et al., 1999). There are no buccal fenestrations and the highly derived dentition lacks primary molars and successional teeth. A more convenient method is now possible. The development of contrast agents that reveal anatomical details holds much promise for analyzing human fetal anatomy. Recently in our lab we have tested the use of phosphotungstic acid staining on whole fetal heads. Several of the same specimens I scanned using the μ CT were rescanned following PTA staining. A high degree of internal detail can be seen (Fig. 4.1A-E’).

Figure 4.1 Comparison of microCT imaging before and after PTA staining

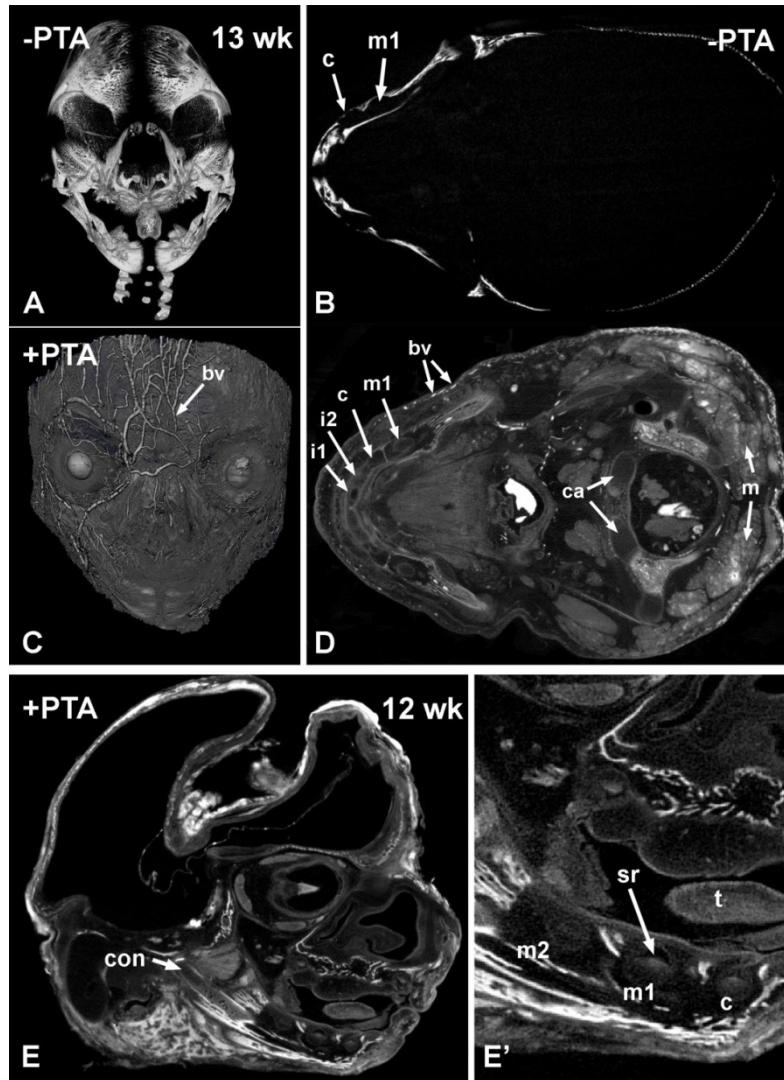


Fig. 4.1 Head to head comparison of the same specimen scanned with conventional micro CT (A,B) and then again after staining with PTA (C,D). A,B) A frontal view of the whole skull and horizontal slice through the mandible as used for this study. The ossified bones of the skull are visible. C) The external reconstructed isosurface shows amazing details of the facial blood vessels (bv). D) The slice view of the head at approximately the same level as in B shows the tooth crypts and follicles within them. Cartilages are easily visible as in the cranial base (ca). The occipital muscles are also visible (m). E,E') parasagittal slices through a 12 week fetus showing the condyle is partially mineralized (con) and each tooth follicle is visible. The details of the enamel organs for m2, m1 and c are visible including the stellate reticulum (sr). The musculature of the head is also easily visible including that of the tongue and (t)

4.4.2 Genetic control of dental crowding

I am just beginning to appreciate the power of 3D morphometrics to reveal shape changes. Many additional analyses are possible such as including the contralateral teeth, landmarking the mandible so that I can reveal where exactly bone shape is changing relative to the teeth. Such detailed analysis has never been done in a human context, except at the level of cells {Radlanski, 2016 #63}. The understanding of how the tooth follicle, the tooth crypt, the alveolar bone and mandible are interrelated may be of clinical importance. I predict that setting up the patterns of tooth alignment for the primary dentition will determine how the permanent dentition is arranged. The correlations between the primary and permanent successional teeth are likely to be very high because they are contained within the same crypts during fetal development. The proportionate growth of the mandible to the teeth may be determined much earlier than originally thought. Finally, the tremendous level of symmetry revealed in my study suggests that it is genetics that determines the sizes, shapes and positions of the teeth rather than environmental factors. My work leads the way for further studies on the molecular controls of follicular growth which now we know has spatially distinct characteristics.

Bibliography

- Alfaqeeh, S. A., Gaete, M. and Tucker, A. S.** (2013). Interactions of the tooth and bone during development. *Journal of Dental Research* **92**, 1129-35.
- Balic, A. and Thesleff, I.** (2015). Tissue Interactions Regulating Tooth Development and Renewal. *Curr Top Dev Biol* **115**, 157-86.
- Bareggi, R., Sandrucci, M. A., Baldini, G., Grill, V., Zweyer, M. and Narducci, P.** (1995). Mandibular growth rates in human fetal development. *Arch Oral Biol* **40**, 119-25.
- Blechsmidt, E.** (1953). [The development of the tooth germ in man dynamic formation of the human embryo]. *Acta Anat (Basel)* **17**, 207-39.
- Cahill, D. R. and Marks, S. C., Jr.** (1980). Tooth eruption: evidence for the central role of the dental follicle. *J Oral Pathol* **9**, 189-200.
- Diewert, V. M.** (1985). Development of human craniofacial morphology during the late embryonic and early fetal periods. *Am J Orthod* **88**, 64-76.
- Diewert, V. M. and Wang, K. Y.** (1992). Recent advances in primary palate and midface morphogenesis research. *Crit Rev Oral Biol Med* **4**, 111-30.
- Dong, X., Shen, B., Ruan, N., Guan, Z., Zhang, Y., Chen, Y. and Hu, X.** (2014). Expression patterns of genes critical for BMP signaling pathway in developing human primary tooth germs. *Histochem Cell Biol* **142**, 657-65.
- Fleischmannova, J., Matalova, E., Sharpe, P. T., Misek, I. and Radlanski, R. J.** (2010). Formation of the tooth-bone interface. *J Dent Res* **89**, 108-15.
- Gondre-Lewis, M. C., Gboluaje, T., Reid, S. N., Lin, S., Wang, P., Green, W., Diogo, R., Fidelia-Lambert, M. N. and Herman, M. M.** (2015). The human brain and face: mechanisms of cranial, neurological and facial development revealed through malformations of holoprosencephaly, cyclopia and aberrations in chromosome 18. *Journal of Anatomy* **227**, 255-67.
- Honda, M. J., Imaizumi, M., Suzuki, H., Ohshima, S., Tsuchiya, S. and Satomura, K.** (2011). Stem cells isolated from human dental follicles have osteogenic potential. *Oral Surg Oral Med Oral Pathol Oral Radiol Endod* **111**, 700-8.
- Juuri, E., Jussila, M., Seidel, K., Holmes, S., Wu, P., Richman, J., Heikinheimo, K., Chuong, C. M., Arnold, K., Hochedlinger, K. et al.** (2013). Sox2 marks epithelial competence to generate teeth in mammals and reptiles. *Development* **140**, 1424-32.
- Kjaer, I. and Bagheri, A.** (1999). Prenatal development of the alveolar bone of human deciduous incisors and canines. *J Dent Res* **78**, 667-72.

- Kristensen, E., Parsons, T. E., Hallgrímsson, B. and Boyd, S. K.** (2008). A novel 3-D image-based morphological method for phenotypic analysis. *IEEE Trans Biomed Eng* **55**, 2826-31.
- Lee, S. H., Bedard, O., Buchtova, M., Fu, K. and Richman, J. M.** (2004). A new origin for the maxillary jaw. *Dev Biol* **276**, 207-24.
- Logan, W. H. C. and Kronfeld, R.** (1933). Development of the human jaws and surrounding structures from birth to the age of fifteen years. *J Am Dent Assoc* **20**, 379-427.
- MacDonald, M. E., Abbott, U. K. and Richman, J. M.** (2004). Upper beak truncation in chicken embryos with the cleft primary palate mutation is due to an epithelial defect in the frontonasal mass. *Dev Dyn* **230**, 335-49.
- Marks, S. C., Jr. and Cahill, D. R.** (1984). Experimental study in the dog of the non-active role of the tooth in the eruptive process. *Arch Oral Biol* **29**, 311-22.
- McBratney-Owen, B., Iseki, S., Bamforth, S. D., Olsen, B. R. and Morriss-Kay, G. M.** (2008). Development and tissue origins of the mammalian cranial base. *Dev Biol* **322**, 121-32.
- Mina, M. and Kollar, E. J.** (1987). The induction of odontogenesis in non-dental mesenchyme combined with early murine mandibular arch epithelium. *Arch Oral Biol* **32**, 123-7.
- Morimoto, N., Ogihara, N., Katayama, K. and Shiota, K.** (2008). Three-dimensional ontogenetic shape changes in the human cranium during the fetal period. *Journal of Anatomy* **212**, 627-35.
- Neumann, K., Moegelin, A., Temminghoff, M., Radlanski, R. J., Langford, A., Unger, M., Langer, R. and Bier, J.** (1997). 3D-computed tomography: a new method for the evaluation of fetal cranial morphology. *J Craniofac Genet Dev Biol* **17**, 9-22.
- Norberg, O.** (1933). Die Morphogenese der primitiven Zahnalveolen beim Menschen und ihre Bedeutung für die Stellungsanomalien der Zähne. *Anat. Embryol. (Berl.)* **100**, 394-432. *Anat. Embryol. (Berl.)* **100**, 394-432.
- O'Rahilly, R. and Muller, F.** (2007). The development of the neural crest in the human. *J Anat* **211**, 335-51.
- O'Rahilly, R. and Müller, F.** (2001). Human embryology & teratology. New York: Wiley-Liss.
- Ooë, T.** (1981). Human Tooth and Dental Arch Development. Tokyo: Ishiyaku Publishers Inc.
- Radlanski, R. J.** (1995). Morphogenesis of human tooth primordia: the importance of 3D computer-assisted reconstruction. *Int J Dev Biol* **39**, 249-56.
- Radlanski, R. J.** (2003a). Development of the dentition: four-dimensional visualization and open questions concerning the morphogenesis of tooth form and occlusion. *Orthod Craniofac Res* **6 Suppl 1**, 82-8.

- Radlanski, R. J.** (2003b). Prenatal craniofacial morphogenesis: four-dimensional visualization of morphogenetic processes. *Orthod Craniofac Res* **6 Suppl 1**, 89-94.
- Radlanski, R. J., Renz, H., Tsengelsaikhan, N., Schuster, F. and Zimmermann, C. A.** (2016). The remodeling pattern of human mandibular alveolar bone during prenatal formation from 19 to 270mm CRL. *Ann Anat* **205**, 65-74.
- Radlanski, R. J., Renz, H., Zimmermann, C. A., Mey, R. and Matalova, E.** (2015). Morphogenesis of the compartmentalizing bone around the molar primordia in the mouse mandible during dental developmental stages between lamina, bell-stage, and root formation (E13-P20). *Ann Anat* **200**, 1-14.
- Radlanski, R. J., van der Linden, F. P. and Ohnesorge, I.** (1999). 4D-computerized visualisation of human craniofacial skeletal growth and of the development of the dentition. *Ann Anat* **181**, 3-8.
- Reid, S. N., Ziermann, J. M. and Gondre-Lewis, M. C.** (2015). Genetically induced abnormal cranial development in human trisomy 18 with holoprosencephaly: comparisons with the normal tempo of osteogenic-neural development. *J Anat* **227**, 21-33.
- Sperber, G. H. and Guttman, G. D.** (2010). Craniofacial embryogenetics and development. Shelton, CT: People's Medical Pub. House USA, 2010.
- Sperber, G. H., Sperber, S. M. and Guttman, G. D.** (2010). Craniofacial embryogenetics and development. Shelton, CT: People's Medical Pub. House USA.
- Thesleff, I.** (2014). Current understanding of the process of tooth formation: transfer from the laboratory to the clinic. *Aust Dent J* **59 Suppl 1**, 48-54.
- Thesleff, I., Keranen, S. and Jernvall, J.** (2001). Enamel knots as signaling centers linking tooth morphogenesis and odontoblast differentiation. *Adv Dent Res* **15**, 14-8.
- Van der Linden, F. P., McNamara, J. A., Jr. and Burdi, A. R.** (1972). Tooth size and position before birth. *J Dent Res* **51**, 71-4.
- Wang, B., Li, H., Liu, Y., Lin, X., Lin, Y., Wang, Y., Hu, X. and Zhang, Y.** (2014). Expression patterns of WNT/beta-CATENIN signaling molecules during human tooth development. *J Mol Histol* **45**, 487-96.
- Wise, G. E. and King, G. J.** (2008). Mechanisms of tooth eruption and orthodontic tooth movement. *J Dent Res* **87**, 414-34.
- Zelditch, M., Swiderski, D. and Sheets, H. D.** (2012). Geometric morphometrics for biologists : a primer. Amsterdam ; London: Elsevier.

Appendix A: Buccal bone description by specimen on right and left sides

ID	Right					Left					RL symmetry
	i1	i2	c	m1	m2	i1	i2	c	m1	m2	
12-1	above bone	above bone	open	open, no me foramen	open	above bone	above bone, bone growing up over buccal	open	open, no me foramen	open	YES
12-2	above bone	above bone	open	partially open with band of diagonal bone across buccal, start of me foramen	closed	above bone	above bone	open	partially open with band of diagonal bone across buccal, start of me foramen	closed	YES
12-3	above bone	above bone	open	mostly open with partial bone exposing MB. Me foramen forming on R	open in centre of buccal	above bone	above bone	open	mostly open with partial bone exposing MB. No me foramen yet but groove is present	open in centre of buccal	YES
13-1	open 2/3 not above bone	closed but occ open, not above bone	open	open, me foramen not formed yet	1/2 open buccal, at level of bone	open 2/3 not above bone	closed, not above bone	open	open, me foramen not formed yet	1/3 open on buccal, at level of bone	YES
13-2	open 2/3 not above bone	closed but occ open, not above bone	open	open, prominent interprox bone between m1 and c, no me foramen yet	Occlusal 1/3 exposed on buccal, slightly more on R than L,	open 2/3 not above bone	closed, not above bone	open	open, interproximal bone only present occlusally between m1 and c, no me foramen yet	Occlusal 1/3 exposed on buccal,	YES

ID	Right					Left					RL symmetry
	i1	i2	c	m1	m2	i1	i2	c	m1	m2	
13-3	open 2/3 not above bone	closed but occ open not above bone	open	open, no me foramen yet	1/2 of buccal surface is exposed, more than on L	open 1/3 not above bone	closed but occ open not above bone	open	open with buccal strip of bone going diagonally across, me foramen starting	open with buccal strip of bone about 1/4 down from occlusal surface	NO
13-4	open	2/3 closed but occ open	open	open, small interprox bone at marginal ridge between m1 and m2 no me foramen	1/2 open with buccal patch	open	2/3 closed but occ open	open	open with small bone island in centre of buccal, otherwise identical to R small interprox bone at marginal ridge between m1 and m2, no me foramen yet	1/2 open with buccal patch	YES
14-1	Above bone, open	Above bone, closed with occ open	open	mostly open, foramen starting but not formed yet. Strip of bone extending from D to M, bottom 1/3 of buccal surface	open in centre of buccal	Above bone	Above bone closed	open	mostly open, me foramen starting, a groove is present in bone, Strip of bone extending from D to M, bottom 1/3 of buccal surface	open in centre of buccal	YES

ID	Right					Left					RL symmetry
	i1	i2	c	m1	m2	i1	i2	c	m1	m2	
14-2	open	closed with occ open and small distal fenestration	open with small bone island on distal	2/3 open with bone projections gingivally, more obvious me foramen on R than L	1/2 open	open	closed with occ open and small distal fenestration	open with small bone island on distal	2/3 open with robust bone projections interproximally. Me foramen not quite as well formed as on R but close	1/2 open	YES
14-3	open	closed with occ open	open	open, me foramen not formed yet	1/2 exposed with bone encroaching from distal	1/2 open with gingival bone projection	closed with occ open	open	2/3 open, me foramen not formed	1/2 exposed (occ gingival height) with small buccal bone fenestration	YES
15-1	open	3/4 closed with occ open	open	open, no me foramen formed yet	bridge of bone from M to D about halfway down buccal surface so different than L	open	3/4 closed with occ open	Open, probably missed interprox bone between i2 and c in segmenting the md	1/2 open with gingival bone fenestration, no me foramen	3/4 of buccal surface exposed	YES but not for m2 so call it a NO
15-2	2/3 open	closed with occ open	open	2/3 open me foramen is formed fully	1/3 open with gingival bone extensions	2/3 open	closed with occ open	3/4 open	2/3 open, me foramen is formed fully	1/3 open with gingival bone extensions	YES

ID	Right					Left					RL symmetry
	i1	i2	c	m1	m2	i1	i2	c	m1	m2	
15-3	open	closed with occ open and distal bone fenestration	open	2/3 open with gingival bone extension, me foramen present surrounded by bone on occlusal side	1/2 open with gingival bone fenestration	open	closed with occ open	open with interproximal bone projections	2/3 open with gingival bone extension, me foramen present surrounded by bone on occlusal side	1/2 open with gingival bone extensions	YES
16-1	open	2/3 closed with small fenestration gingivally and occ open with bone outgrowths	open but with growth interproximally	open with growth interproximally and around the edges, no me foramen yet	2/3 closed with band of buccal bone and gingival fenestration	open	2/3 closed with small fenestration gingivally and occ open	open but with growth interproximally	open with growth interproximally and around the edges, no me foramen yet	2/3 closed but growth around the edges	YES
16-2	open	closed but with some bone fenestrations distally and gingivally and occ open	open	open with minimal bone growth from the edges, me foramen is present	1/2 open with gingival bone extension	open	closed but with some bone fenestrations distally and gingivally and occ open	open	open but band of buccal bone gingivally surrounding the me foramen so it is present	1/2 open with gingival bone extension	YES

ID	Right					Left					RL symmetry
	i1	i2	c	m1	m2	i1	i2	c	m1	m2	
16-3	open, 1/3 above bone	closed with occ open	open	partial, band of bone across buccal surface (1/3 from gingival margin) Me foramen is almost formed	open on buccal, 2/3 of crown exposed gingival bone growth	open, 1/3 above bone	closed with occ open	open	partial, band of bone across buccal surface (1/3 from gingival margin) Me foramen has formed	open on buccal, 2/3 of crown exposed	YES
17-1	open	closed with minimal buccal bone fenestrations distally. Occ open	open but with bone growth interproximally and around the edges	2/3 open but with bone growth interproximally and around the edges. Mental foramen well formed	1/3 open but with bone growth interproximally and around the edges	open	closed with buccal bone fenestrations distally. Occ open	open but with bone growth interproximally and around the edges	2/3 open but with bone growth interproximally and around the edges. Bone fenestration gingivally. Me foramen well formed	1/3 open but with bone growth interproximally and around the edges with very small buccal bone fenestration	YES
17-2	open	buccal bone fenestrations	open	2/3 open with bone extension from the gingival aspect. Me foramen formed	1/2 open with bone extension from the gingival aspect	open	buccal bone fenestrations	open	2/3 open with bone extension from the gingival aspect. Me foramen formed	1/2 open with bone extension from the gingival aspect	YES

ID	Right					Left					RL symmetry
	i1	i2	c	m1	m2	i1	i2	c	m1	m2	
17-3	2/3 open with bone growth around edges	closed with buccal bone fenestrations distally and small fenestration buccally	Open with some interproximal and gingival growth	1/2 open with buccal bone growth around edges and bone fenestration mesio gingivally. Mental foramen is well formed	1/2 open with buccal bone growth around edges	open	closed with buccal bone fenestrations distally	Open with some interproximal and gingival growth	1/2 open with buccal bone growth around edges and bone fenestration mesio gingivally. Mental foramen well formed	1/2 open with buccal bone growth around edges	yes
18-1	2/3 open with bone growth around edges	closed with occ open and bone fenestrations occlusally	Open with some interproximal and gingival growth	2/3 open with some interproximal and gingival growth with gingival fenestration (mental foramen). Mental foramen formed	1/3 open with some interproximal and gingival growth	2/3 open with bone growth around edges	closed with occ open and bone fenestrations occlusally	open	2/3 open with some interproximal and gingival growth with gingival fenestration (mental foramen). Mental foramen formed	1/3 open with some interproximal and gingival growth	YES
18-2	open	2/3 open with buccal bone growth	open	open. Mental foramen present but not as well formed as on the L	2/3 exposed with no bone crossing the buccal surface like on L	open	2/3 open with buccal bone growth	open	2/3 exposed with bone coming from D towards M. Mental foramen well formed.	1/2 open with thin band of bone across buccal at level of gingival 1/3	No

ID	Right					Left					RL symmetry
	i1	i2	c	m1	m2	i1	i2	c	m1	m2	
18-3	open	2/3 open with buccal bone growth	open	a band of bone is growing across from D, has made contact mesially unlike on the L side. Me foramen present	2/3 open with bone growth around margins	open	2/3 open with buccal bone growth	open	Mostly exposed but a band of bone is growing across from D, has not made contact mesially. Me foramen present	2/3 open with bone growth around margins	No
19-1	open	closed with occ open	open with marginal bone growth	1/2 open with buccal bone growth around edges and bone fenestration mesiogingivally (mental foramen) Mental foramen formed	1/3 open with bone growth around margins	open	closed with occ open	open with marginal bone growth	1/2 open with buccal bone growth around edges and bone fenestration mesiogingivally (mental foramen) Me foramen formed	1/3 open with bone growth around margins	YES
19-2	open	closed with occ open	open	1/3 open with bone growth around margins with band of bone extension across buccal surface. Me foramen incomplete	1/3 open with bone growth around margins	open	closed with occ open	open	1/3 open with bone growth around margins with band of bone extension across buccal surface. Me foramen incomplete	1/3 open with bone growth around margins	YES

ID	Right					Left					RL symmetry
	i1	i2	c	m1	m2	i1	i2	c	m1	m2	
19-3	open	closed	open but bone is starting to encroach from M and D	occlusal 2/3 open, not above bone anymore, little fenestration on MB corner. Mental foramen visible, very thick bone around the foramen	occl 1/3 open not above bone	open	closed	open but bone is starting to encroach from M and D	occlusal 2/3 open, not above bone anymore, little fenestration on MB corner. Mental foramen present, very thick bone around the foramen	occl 1/3 open not above bone	YES